

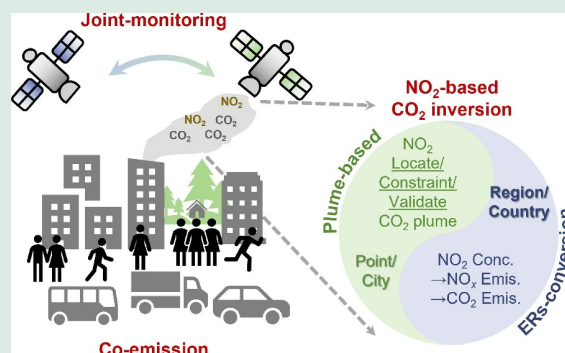
Monitoring fossil fuel CO₂ emissions from co-emitted NO₂ observed from space: progress, challenges, and future perspectives

Hui Li^{1,2,#}, Jiabin Qiu^{1,2,#}, Kexin Zhang^{1,2}, Bo Zheng ^{1,2}

1. Shenzhen Key Laboratory of Ecological Remediation and Carbon Sequestration, Institute of Environment and Ecology, Tsinghua Shenzhen International Graduate School, Tsinghua University, Shenzhen 518055, China
2. State Environmental Protection Key Laboratory of Sources and Control of Air Pollution Complex, Beijing 100084, China

HIGHLIGHTS


- CO₂ emission monitoring supports achieving Nationally Determined Contributions.
- Co-emitted NO_x and CO₂ in fuel combustion enable NO₂-based CO₂ emission inversion.
- Structural and data uncertainties challenge researchers but guide future pathway.
- Interdisciplinary collaboration is crucial for advancing CO₂ emission inversion.



ABSTRACT: Developing an anthropogenic carbon dioxides (CO₂) emissions monitoring and verification support (MVS) capacity is essential to support the Global Stocktake (GST) and ratchet up Nationally Determined Contributions (NDCs). The 2019 IPCC refinement proposes top-down inversed CO₂ emissions, primarily from fossil fuel (FFCO₂), as a viable emission dataset. Despite substantial progress in directly inferring FFCO₂ emissions from CO₂ observations, substantial challenges remain, particularly in distinguishing local CO₂ enhancements from the high background due to the long atmospheric lifetime. Alternatively, using short-lived and co-emitted nitrogen dioxide (NO₂) as a proxy in FFCO₂ emission inversion has gained prominence. This methodology is broadly categorized into plume-based and emission ratios (ERs)-based inversion methods. In the plume-based methods, NO₂ observations act as locators, constraints, and validators for deciphering CO₂ plumes downwind of sources, typically at point source and city scales. The ERs-based inversion approach typically consists of two steps: inferring NO₂-based nitrogen oxides (NO_x) emissions and converting NO_x to CO₂ emissions using CO₂-to-NO_x ERs. While integrating NO₂ observations into FFCO₂ emission inversion offers advantages over the direct CO₂-based methods, uncertainties persist, including both structural and data-related uncertainties.

These authors contributed equally to this work.

Special Issue—Young Talent

 Corresponding author. E-mail: bozheng@sz.tsinghua.edu.cn

Article history: Received 25 May 2024, Revised 4 July 2024, Accepted 19 August 2024, Available online 18 October 2024

©The Author(s) 2025. This article is published with open access at link.springer.com and journal.hep.com.cn

Addressing these uncertainties is a primary focus for future research, which includes deploying next-generation satellites and developing advanced inversion systems. Besides, data caveats are necessary when releasing data to users to prevent potential misuse. Advancing NO₂-based CO₂ emission inversion requires interdisciplinary collaboration across multiple communities of remote sensing, emission inventory, transport model improvement, and atmospheric inversion algorithm development.

KEYWORDS: Fossil fuel CO₂ emissions, CO₂ satellites, NO₂ satellites, Emission inversion methods, Uncertainty management, Future perspectives

1 Introduction

On November 17, 2023, the ERA5 (ECMWF Reanalysis v5) data (Hersbach et al., 2020) recorded a temporary exceedance of the 2 °C global warming, underscoring the urgent need to address climate change. Over recent decades, the detrimental effects of climate change have become increasingly evident, with a marked rise in the frequency and intensity of extreme weather events, including downpours, droughts, and wildfires (Swain et al., 2020; Newman and Noy, 2023; Ombadi et al., 2023; Yuan et al., 2023). In response to this critical global challenge, most nations have committed to reducing greenhouse gas emissions through Nationally Determined Contributions (NDCs) as stipulated by the Paris Agreement. These commitments, updated every five years since 2020, constitute a crucial part of the global effort to combat climate change (Röser et al., 2020). To timely evaluate collective progress toward limiting global warming to below 2 °C (ideally 1.5 °C) and motivate parties to ratchet up their NDCs, the Global Stocktake (GST) was initiated in 2023 and will recur every five years (Editorial, 2023). Rigorous and comprehensive implementation of NDCs could potentially constrain global warming to just under 2 °C, which emphasizes the necessity for intensified and unequivocal actions from all participating entities (Meinshausen et al., 2022).

To bolster climate ambitions, the development of anthropogenic carbon dioxides (CO₂) Emissions Monitoring & Verification Support (MVS) capacity is essential (European et al., 2017). Anthropogenic CO₂ emissions are primarily categorized into two sources: fossil fuel combustion and land use, accounting for 88.1% and 11.9% of emissions, respectively, according to the Global Carbon Budget 2023 (Friedlingstein et al., 2023). Given the dominance of fossil fuel CO₂ emissions (FFCO₂), the quest for a thorough comprehensive understanding of FFCO₂ emissions has spurred numerous research endeavors (Jones et al., 2023; Liu et al., 2023). The 2006 IPCC Guidelines for National Greenhouse Gas Inventories (IPCC, 2006) identified

bottom-up inventory compilation as the primary method for countries to report their estimated emissions. However, the bottom-up method entails substantial labor and time investment in acquiring detailed data on activity levels and emission factors. These requirements pose challenges for many countries, particularly those grappling with the development of reliable statistical databases. In contrast, advancements in satellite remote sensing technologies have provided indispensable tools for monitoring changes in atmospheric composition concentrations (Yang et al., 2013). Concurrently, inversion algorithms for deriving emissions from satellite-observed column concentrations have flourished. In this context, the top-down emission inversion was proposed as an alternative to the bottom-up approach in the 2019 Refinement to 2006 IPCC Guidelines (Eduardo Calvo Buendia et al., 2019). The top-down inverted emissions have been currently recognized and adopted as a viable method for international climate commitments.

Researchers have dedicated considerable effort to developing top-down FFCO₂ emission inversions directly from CO₂ satellite observation, broadly categorized into data-driven (e.g., cross-sectional flux method (CSF)) and model-driven approaches (e.g., based on Lagrangian or Eulerian models) (Nehrkorn et al., 2010; Nassar et al., 2017). CO₂-based inversions have been widely adopted to infer FFCO₂ emissions from point and city scales, demonstrating their feasibility. However, persistent challenges remain despite these advances. For instance, natural fluxes exhibit substantial spatial and seasonal fluctuations, whereas FFCO₂ emissions remain relatively stable, complicating the detection of CO₂ enhancement signals from human activities (Buchwitz et al., 2021; Byrne et al., 2023). To address these limitations, integrating co-emitted short-lived proxies such as nitrogen dioxides (NO₂) into CO₂ emission inversions has recently emerged as an effective approach (Berezin et al., 2013; Reuter et al., 2014).

Amidst the rapid advancements in FFCO₂ emission inversion methodologies, there is a critical need for a

comprehensive and systematic review to consolidate existing knowledge and guide future research endeavors. This review aims to synthesize the current research progress and challenges in FFCO₂ emission inversions. It is noteworthy that, unless otherwise specified, the CO₂ emissions in this study refer to FFCO₂ emissions. This paper is organized as follows: Section 2 provides an overview of CO₂ emission inversion methods from CO₂ satellite observations including both advantages and limitations; Section 3 summarizes CO₂ emission inversion methods integrating NO₂ retrievals, detailing the principles and applications; Section 4 examines the inherent limitations and uncertainties within current NO₂-based CO₂ emission inversion frameworks; Section 5 outlines potential future research directions for both technology and methodology for this field; and finally, Section 6 offers conclusions.

2 Utilizing satellite CO₂ data to monitor CO₂ emissions

2.1 CO₂ monitoring satellites

Over the past two decades, substantial progress has been made in satellite monitoring of CO₂ column concentrations, providing a robust data foundation for CO₂ emission inversion (Table 1). The European Space Agency (ESA) launched the Environmental Satellite (Envisat) in 2002, equipped with the Scanning Imaging Absorption Spectrometer for Atmospheric Chartography (SCIAMACHY), enabling the monitoring of various atmospheric compositions (Burrows et al., 1995; Bovensmann et al., 1999). Until 2009, Envisat remained the sole satellite capable of measuring column-averaged dry-air mole fractions of carbon dioxide (XCO₂), providing long-term data on the global distribution of atmospheric CO₂ concentrations (Schneising et al., 2011). In 2009, the Japan Aerospace Exploration Agency launched the Greenhouse gases Observing SATellite (GOSAT), the first satellite dedicated to monitoring CO₂ and methane (CH₄) concentration (Kuze et al., 2009). Building on the success of GOSAT, Japan launched the GOSAT-2 in 2018, featuring the advanced Fourier Transform Spectrometer-2 (TANSO-FTS-2) and the Cloud and Aerosol Imager-2 (TANSO-CAI-2), substantially expanding coverage of the shortwave infrared spectrum. These advancements are particularly beneficial for reducing interference in CO₂ inversion caused by clouds and aerosols, thereby improving observation accuracy (Suto et al., 2021).

Since 2014, satellites have been substantially

advanced in achieving finer resolution and reducing uncertainty, thereby enhancing their ability to detect CO₂ signals. The Orbital Carbon Observing-2 (OCO-2), launched by the National Aeronautics and Space Administration (NASA) in 2014, utilizes three high-resolution grating spectrometers to achieve precise CO₂ measurements (Crisp et al., 2017). It plays a pivotal role in assessing the gross primary productivity and carbon budgets of terrestrial ecosystems by revealing seasonal and regional variations in CO₂ concentrations and Solar-induced chlorophyll fluorescence (SIF) (Sun et al., 2017). OCO-2 can provide unique insights into the complex interactions between climate phenomena (e.g., El Niño events) and natural disasters (e.g., wildfires) within the global carbon cycle (Chatterjee et al., 2017; Liu et al., 2017). Furthermore, it demonstrates the potential to characterize CO₂ emission hotspots from both anthropogenic and natural sources (Eldering et al., 2017; Heymann et al., 2017; Schwandner et al., 2017). Despite these technological advancements, uncertainty persists among different satellites, such as GOSAT and OCO-2, which differ in spatial coverage, data amount, and retrieval biases (Wang et al., 2019). To enhance the monitoring capabilities of CO₂ in the atmosphere, NASA launched and hosted the Orbiting Carbon Observatory-3 (OCO-3) sensor on the International Space Station in 2019. Its Snapshot Area Map (SAM) and target mode measurements can scan larger contiguous areas and capture plume structures over city areas more effectively compared to OCO-2 (Eldering et al., 2019).

The Chinese CO₂ satellite TanSat was launched in 2016. The CO₂ retrieval data was first utilized to map global CO₂ distribution (Yang et al., 2018). Liu et al. (2018) pioneered efforts to validate TanSat retrieval against eight ground-based measurements from the Total Carbon Column Observing Network (TCCON), demonstrating a precision of 2.11 ppm. Subsequent endeavors have persistently aimed at refining TanSat data precision through spectral calibration and algorithm optimization, achieving retrievals with a precision of 1.47 ppm, comparable to OCO-2 (Yang et al., 2020; Hong et al., 2022). Building upon these advancements, Hong et al. (2024) further improved TanSat XCO₂ retrievals by implementing spectral recalibration, spectral window optimization, and explicit radiative transfer simulation. This work extended the utility of TanSat data to capture CO₂ enhancements over the ocean and quantify emission flux.

2.2 Data- and model-driven approaches

The initial mission of CO₂ satellites is to assess carbon

Table 1 Summary of major CO₂ monitoring satellites since 2000

Satellite	Envisat ^a	GOSAT ^b	OCO-2	TanSat	GOSAT-2	OCO-3
Instrument	SCIAMACHY	TANSO-FTS/ TANSO-CAI	Three high-resolution grating spectrometers	ACGS/ CAPI	TANSO-FTS-2/ TANSO-CAI-2	Three high-resolution grating spectrometers
Launch date	Mar 01, 2002	Jan 23, 2009	Jul 02, 2014	Dec 21, 2016	Oct 29, 2018	May 04, 2019
Country/Region	Europe	Japan	United States	China	Japan	United States
Agency	ESA	JAXA/MOE	NASA	MOST/CAS/CMA	JAXA/MOE	NASA
Monitoring gas species	O ₃ , N ₂ O, CH ₄ , CO ₂ , H ₂ O	CO ₂ , CH ₄ , H ₂ O	CO ₂	CO ₂	CO ₂ , CH ₄ , CO	CO ₂
Observation modes	Nadir, Limb, Sun and Moon Occultation	Nadir, Glint, Target	Nadir, Glint, Target	Nadir, Glint, Target	Nadir, Glint, Target, Limb	Nadir, Glint, Target, SAM
Pixel resolution (km ²)	30 × 60	~10 × 10	1.29 × 2.25	2 × 2	~10 × 10	1.6 × 2.2
Repeat cycle (d)	35	3	16	16	6	Variable
Overpass time (LT)	10:00 ± 0:05	13:00 ± 0:15	~13:15	~13:30	13:00 ± 0:15	Variable
Accuracy (ppm)	14	4	< 1	< 4	0.5	< 1
Altitude (km)	799	666	705	712	613	400
Inclination (°)	98.55	98.06	98.20	98.16	97.84	51.60

*Abbreviations: JAXA (Japan Aerospace Exploration Agency); MOE (Ministry of the Environment); MOST (Ministry of Science and Technology); CAS (Chinese Academy of Sciences); CMA (China Meteorological Administration). Detailed data sources are provided in Table S1 in SI.
^a Envisat satellite ceased its operations on Apr 08, 2012, when communication with the satellite was unexpectedly lost.
^b GOSAT transferred to the least load mode and all the instrument and data recorders were shut down on May 17, 2018.

budgets on a large spatial scale, while advancements in spatial resolution and signal-to-noise ratios have demonstrated their potential for quantifying FFCO₂ local emissions (Wu et al., 2020; Nassar et al., 2021). Currently, there are two main methods for estimating FFCO₂ emissions from CO₂ satellites: data-driven and model-driven approaches (Table 2).

Data-driven methods typically involve processing satellite XCO₂ along with local wind field information, which is suitable for estimating emissions from large point sources (e.g., power plants) and isolated cities assuming steady-state conditions (Velazco et al., 2011; Nassar et al., 2022). These methods primarily include four categories (Table 2), generally starting with the detection of CO₂ plumes from satellite imagery to determine regions for emission quantification and attribution. Plumes can be identified using segmentation algorithms (Dumont Le Brazidec et al., 2023) or thresholding based on signal-to-noise ratio (Kuhlmann et al., 2021). Plume positioning can also be achieved using known source locations and wind fields (Lin et al., 2023). Quantifying XCO₂ enhancements above the background entails carefully defining and deducting the background levels. Various approaches have been employed for this purpose, such as smoothing the background field with low-pass filters (Thoning et al., 1989), estimating the background based on the upwind direction of point source emissions (Kort et al., 2012), and incorporating background term into a linear polynomial (Reuter et al., 2019). The identified XCO₂

enhancements above the background levels are finally combined with local wind field data to estimate emissions related to these enhancements. Data Science and Artificial intelligence (AI) techniques, such as clustering analysis and convolutional neural network (CNN), have been increasingly integrated into data-driven methods to extract emission information from concentration distributions and enhance the efficiency of data processing (Schuit et al., 2023).

Model-driven methods generally involve the utilization of Eulerian (e.g., Weather Research and Forecasting-Chem (WRF-Chem)) (Lei et al., 2021) and Lagrangian models (e.g., Column-Stochastic Time-Inverted Lagrangian Transport model (X-STILT)) (Wu et al., 2020), which are commonly employed for city or regional-scale CO₂ emission inversion. Eulerian models utilize fixed grid cells and a known prior emission inventory to simulate XCO₂ by forwardly transporting emitted CO₂ molecules through the simulation domain. Lagrangian models trace the backward trajectory of air parcels from a given receptor location (e.g., the position of observed XCO₂ enhancement from satellite) to determine the source emission area or footprint contributing to the concentration at the receptor. These models simulate the transport of CO₂ and establish the relationship between CO₂ emissions and satellite-observed XCO₂ concentrations. Pillai et al. (2016) utilized the Bayesian inversion approach, which minimizes the cost function accounting for model- and observation-specific errors, yielding a posterior

Table 2 Overview of commonly used CO₂ emission inversion methods

Category	Method	Main formula/Model	Parameter/Input	Case study
Data-driven	Gaussian plume method (GP)	$V(x,y) = \frac{Q}{\sqrt{2\pi}\sigma(x)} e^{-\frac{y^2}{2\sigma^2(x)}}$	$V(x,y)$: Vertical column x : Distance parallel to the wind direction y : Distance perpendicular to the wind direction Q : Emission flux $\sigma(x)$: Standard deviation	Nassar et al. (2017)
	Cross-sectional flux method (CSF)	$E = U \oint_a^b \Delta\Omega(x,y) dy$	E : Emission rate $\Delta\Omega$: XCO ₂ enhancements relative to background U : Wind speed	Reuter et al. (2019)
	Integrated mass enhancement method (IME)	$E = \frac{U_{eff} \times IME}{L}$	E : Emission rate IME : Integrated mass enhancement above the background U_{eff} : Effective wind speed L : Radial plume length	Cusworth et al. (2023)
	Divergence method (Div)	$E = \nabla F + S$	E : Emission rate ∇F : Divergence of flux S : Sinks	Hakkarainen et al, (2022)
Model-driven	Eulerian models	WRF-Chem/ WRF-GHG	Reanalysis of wind fields/ Prior emissions	Pillai et al. (2016)
	Lagrangian models	STILT/XSTILT/ FLEXPART/HYSPLIT	Reanalysis of wind fields/ Prior emissions	Wu et al. (2020)

estimate of CO₂ emissions. Zheng et al. (2019) applied a maximum likelihood estimation approach to directly estimate CO₂ emissions from XCO₂ observations without prior emission information, by calculating the Jacobian matrix.

2.3 Application in point source and city emissions

Satellite XCO₂ images have been utilized to estimate CO₂ emissions from both point sources and city scales. Regarding point sources, Bovensmann et al. (2010) proposed a conceptual technique (GP method) to quantify CO₂ emissions from power plants based on the Observing System Simulation Experiment (OSSE). Nassar et al. (2017) quantified CO₂ emissions from 7 large and middle-sized power plants based on OCO-2 CO₂ observations and subsequently improved their methods to capture emissions from more point sources (Nassar et al., 2021). Utilizing a high-resolution WRF-Chem model with a spatial resolution of 1.33 km × 1.33 km, Zheng et al. (2019) successfully captured emissions from 7 point sources identified by Nassar et al. (2017), without prior information on emissions from these point sources. Considering the difficulty of accurately detecting XCO₂ enhancements, Reuter et al. (2019) identified XCO₂ enhancements using NO₂ tropospheric vertical column densities (TVCDs) from TROPOspheric Monitoring Instrument (TROPOMI) as a proxy, and then estimated CO₂ emissions from point sources using the CSF method. Cusworth et al. (2023) detected plumes worldwide from OCO-3 and estimated emissions from the world’s largest coal-fired power plants using the IME method. The Divergence (Div)

method has demonstrated potential for estimating CO₂ point source emissions based on Copernicus Anthropogenic Carbon Dioxide Monitoring (CO2M) observations in the future (Hakkarainen et al., 2022).

For city-scale CO₂ emission inversion, Nehrkorn et al. (2010) integrated the Weather Research and Forecasting (WRF) model with the Stochastic Time-Inverted Lagrangian Transport (STILT) model, a Lagrangian Particle Dispersion Model and demonstrated the model’s capability in capturing regional CO₂ fluxes. Wu et al. (2018) developed a modified version of the STILT model, “X-STILT”, which was used to estimate per capita CO₂ emissions from OCO-2 XCO₂ for 20 cities across multiple continents (Wu et al., 2020). Zheng et al. (2020a) used the light cross-sectional flux (LCSF) method focusing on the XCO₂ enhancements detected in satellite images, capturing emissions from 46 cities and industrial areas in China. Chevallier et al. (2020) extended the approach of Zheng et al. (2020a) to the global context and investigated the changes in global CO₂ emissions during the Coronavirus disease 2019 (COVID-19) pandemic. Ye et al. (2020) optimized the ability of FFCO₂ emission estimation based on OCO-2 satellite observations in urban areas by combining a high-resolution chemical transport model (CTM) and multiple OCO-2 tracks. Lei et al. (2021) evaluated the ability of three emission estimation methods (WRF-Chem, X-STILT, CSF method) to detect trends in urban fossil fuel CO₂ emissions and found that Open-Data Inventory for Anthropogenic Carbon dioxide (ODIAC) may have underestimated Lahore’s FFCO₂ emissions.

2.4 Challenges in monitoring large-scale emissions

Although CO₂ satellites hold promise in quantifying point sources and urban CO₂ emissions, substantial challenges persist in their regional and global scale application due to the satellite's capability limitations, such as narrow swath width, low revisit frequency, and cloud interference (Zheng et al., 2019; Santaren et al., 2021).

The limited sampling coverage hinders the identification of CO₂ enhancements over broader coverage. Chevallier et al. (2022) merged a 7-year dataset from OCO-2 with data from the OCO-3 satellite. Their findings only cover about one-third of global CO₂ emissions. There is a critical need for the development of CO₂ detection satellites with wider swath coverage and higher data density to enhance global monitoring capabilities. Additionally, current satellites only capture CO₂ concentrations during their overpass times, which may not necessarily align with actual XCO₂ enhancements considering daily variation. This discrepancy complicates CO₂ emission inversion (Ye et al., 2020). Moreover, the emission inversion method also has potential limitations. Data-driven methods typically assume stable atmospheric conditions and relatively flat terrain, making them more suitable for point sources or urban scales, while the expensive computational costs associated with the model-driven methods may limit their application.

The insensitivity of CO₂ concentration to anthropogenic emission variations and the cloud's impact on CO₂ sensing coverage further complicates the CO₂-based FFCO₂ emission inversion. Weir et al. (2021) pointed out that the OCO-2 satellite has limited capacity to distinguish between changes in anthropogenic emissions and biosphere changes. The minor CO₂ fluctuations resulting from human activities (several ppm) are notably smaller than the background field (~400 ppm), typically falling within the margin of satellites' observation error (Eldering et al., 2017). During the COVID-19 pandemic, a valuable opportunity to investigate the response of atmospheric CO₂ concentrations to human activity changes, the decline in CO₂ observed from satellites was not as pronounced (Buchwitz et al., 2021) compared to the decline in CO₂ emissions (Liu et al., 2022). Chevallier et al. (2020) also illustrated the difficulty in identifying large-scale decreases in CO₂ concentrations due to FFCO₂ emissions during the COVID-19 pandemic. Some key regions such as Hubei Province in China and the Bay of Bengal in India are shrouded in clouds, hindering effective CO₂ concentration observation and emission monitoring. Over sunny areas, yearly

variations in cloud cover can still obscure the detection of CO₂ emission changes (Chevallier et al., 2020).

3 Satellite NO₂-based CO₂ emission monitoring

3.1 NO₂ satellites and NO_x emission inversion

NO₂ satellites have undergone rapid and substantial advancements in recent decades (Table 3). The Global Ozone Monitoring Experiment (GOME), launched in 1995, was a pioneer in global NO₂ observations (Burrows et al., 1999). Successive satellites, including GOME-2A, GOME-2B, and GOME-2C, have since been launched, toward enhanced spatial resolution, advanced data processing algorithms, and broader spatial coverage (Hassinen et al., 2016). The SCIAMACHY, launched in 2002 and initially designed for ozone monitoring, has also been utilized to detect NO₂ columns. In 2014, NASA and the Royal Netherlands Meteorological Institute (KNMI) collaborated to launch the Ozone Monitoring Instrument (OMI), which improved spatial resolution to 13 km × 24 km (Levelt et al., 2006). This technological progress considerably enhanced the capability to resolve NO₂ distribution at fine scales like cities. The launch of TROPOMI in 2017 further advanced this ability, offering a resolution of 7 km × 3.5 km (5.5 km × 3.5 km since 2019) (Veeffkind et al., 2012). In May 2018, China launched the Environmental Trace Gases Monitoring Instrument (EMI) onboard the GaoFen-5 satellite. Zhang et al. (2020) optimized the retrieval algorithm, demonstrating that EMI NO₂ vertical column densities (VCDs) perform comparably to those of OMI and TROPOMI. This satellite has also shown potential in quantifying point source CH₄ emissions (He et al., 2024b). These satellites operate in sun-synchronous polar orbits, crossing the equator at approximately the same local times each day to deliver regular imagery.

Geostationary satellites, positioned above the equator, offer extensive temporal coverage, which enables monitoring of daily atmospheric concentration variations. Geostationary satellites continuously observe the same region of the Earth's surface, covering approximately one-third of it. For instance, the Geostationary Environment Monitoring Spectrometer (GEMS) (Kim et al., 2020b), launched by the Republic of Korea in 2020, has been monitoring atmospheric compositions over East Asia. NASA's Tropospheric Emissions: Monitoring of Pollution (TEMPO), launched in 2023, has been providing hourly observations of atmospheric concentrations in North America (Zoogman et al.,

Table 3 Summary of major NO₂ monitoring satellites over the past three decades

Satellite	Instrument	Launch date	Agency	Monitored gas species	Altitude (km)	Nadir pixel (km ²)	Repeat cycle (d)	Overpass time (LT)
Polar-orbiting								
ERS-2	GOME ^a	Apr 21, 1995	ESA	NO ₂ , O ₃ , BrO, OClO, SO ₂	785	320 × 40	3	~10:30
Envisat	SCIAMACHY ^b	Mar 01, 2002	ESA	NO ₂ , O ₃ , BrO, SO ₂ , HCHO, OClO, H ₂ O/HDO, CH ₄ , CO, CO ₂	799	30 × 215	35	10:00 ± 0:05
Aura	OMI	Jul 15, 2004	NASA	NO ₂ , BrO, HCHO, O ₃ , OClO, SO ₂	705	13 × 24	1	13:45 ± 0:05
Metop-A	GOME-2A ^c	Oct 19, 2006	EUMETSAT/ESA	NO ₂ , O ₃ , SO ₂ , BrO, HCHO, H ₂ O	827	80 × 40	1	~7:50
Metop-B	GOME-2B	Sep 17, 2012	EUMETSAT/ESA	NO ₂ , O ₃ , SO ₂ , BrO, HCHO, H ₂ O	830	80 × 40	1	~9:30
Metop-C	GOME-2C	Nov 07, 2018	EUMETSAT/ESA	NO ₂ , O ₃ , SO ₂ , BrO, HCHO, H ₂ O	827	80 × 40	1	~9:30
Sentinel-5P	TROPOMI	Oct 13, 2017	ESA/NSO	NO ₂ , O ₃ , SO ₂ , CO, CH ₄ , HCHO	824	5.5 × 3.5 ^d	1	~13:30
GaoFen-5	EMI	May 09, 2018	SAST	NO ₂ , SO ₂ , O ₃	706	12 × 13	1	~13:30
Geostationary								
GEO-Kompsat-2B	GEMS	Feb 18, 2020	KMA/KARI/NIER/MLTM	NO ₂ , O ₃ , SO ₂ , HCHO	35786	7 × 8	–	–
Intelsat 40e	TEMPO	Apr 07, 2023	NASA	NO ₂ , O ₃ , HCHO	35786	2 × 4.75	–	–
MTG-S	Sentinel-4/UVN	2024 (Scheduled)	ESA	NO ₂ , O ₃ , SO ₂ , HCHO, CHOCHO	–	8 × 8	–	–

^a GOME ceased operations in November 2021 when ESA decommissioned the ERS-2 satellite.
^b SCIAMACHY ceased operations in April 2012 when contact with the Envisat satellite was lost.
^c GOME-2A ceased operations in June 2011 when Metop-A was decommissioned.
^d On August 06, 2019, the nadir ground pixel dimensions of TROPOMI reduced from 7.0 km × 3.5 km to 5.5 km × 3.5 km.
* Abbreviations: EUMETSAT (European Organisation for the Exploitation of Meteorological Satellites); NSO (Netherlands Space Office); SAST (Shanghai Academy of Spaceflight Technology); KMA (Korea Meteorological Administration); KARI (Korea Aerospace Research Institute); NIER (National Institute of Environmental Research); MLTM (Ministry of Land, Transport and Maritime Affairs). Detailed data sources are provided in Table S2 in SI.

2017). In the near future, the ESA plans to launch Sentinel-4 to monitor air quality across Europe (Ingmann et al., 2012). The progress in remote sensing of NO₂ tends to have outpaced that of CO₂, featuring increased satellite revisit frequencies, finer spatial resolutions, broader coverage, and improved signal-to-noise ratios in column retrievals (Cooper et al., 2022; MacDonald et al., 2023). These advantages render satellite NO₂ retrievals highly effective for constraining nitrogen oxides (NO_x, sum of NO and NO₂) emission inversions. Research and methodologies (Fig. 1) in this field have proliferated over the past two decades. The Mass Balance (MB) method, proposed by Martin et al. (2003), employs a three-dimensional CTM to establish a linear localized response function between NO₂ TVCDs and surface NO_x emissions by grid. It then infers posterior NO_x emissions based on satellite observations and prior emissions. This method simplifies atmospheric transport and nonlinear chemistry to some extent and has proven feasible for inferring daily emission changes on a regional scale (Zhao and Wang, 2009; Gu et al., 2014). However, it is not appropriate for high spatial resolution due to the

inter-grid transport and nonlinear chemistry of NO₂ in the atmosphere. The four-dimensional variational (4D-Var) (Stavrakou et al., 2008) and the Ensemble Kalman Filter (EnKF) method (Miyazaki et al., 2017) utilize data assimilation techniques to minimize the gap between observations and model simulations by adjusting the CTM initial conditions and emissions input. These methods account for atmospheric transport and nonlinear chemistry but require multiple iterations of simulations with high computational costs. To avoid the limitations associated with CTM, researchers have proposed several simplified models to expedite NO_x emission estimation, such as the Exponential Modified Gaussian (EMG), Div, and Peking University High-resolution Lifetime-Emission-Transport (PHLET) methods. These approaches integrate satellite-monitored NO₂ column concentrations with wind fields to update NO_x emissions at high spatial resolutions on a monthly or annual basis. In the EMG method, NO_x emissions are estimated by integrating wind speed with NO₂ line density based on different wind directions, assuming that downwind NO₂ TVCDs from a point source follow a Gaussian distribution. This method has been widely used to quantify emissions from isolated

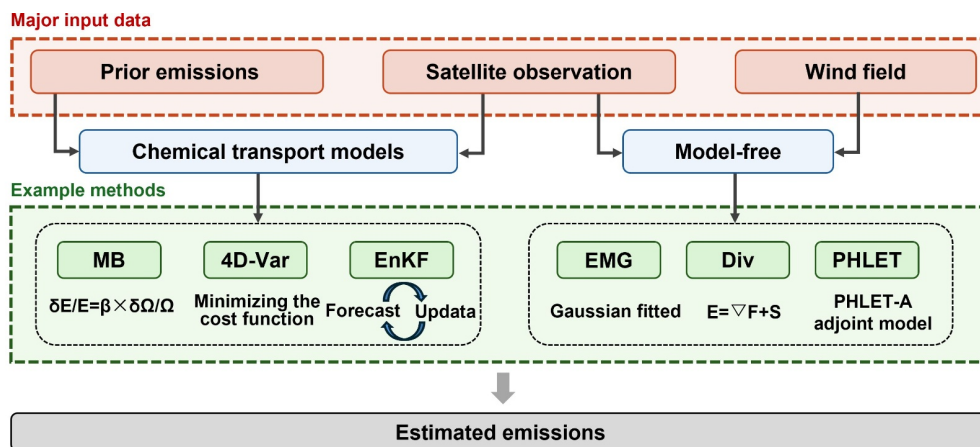


Fig. 1 Overview of NO_x emission inversion methods.

point sources like power plants (Beirle et al., 2011; Liu et al., 2016; Goldberg et al., 2019b). The Div method defines the divergence of flux (F) as the difference between emissions (E) and sinks (S) ($\nabla F = E - S$), creating a vector field of flux by multiplying the wind field with NO₂ columns. The finite difference method is then used to calculate the divergence of this flux field, with peak fitting employed to infer annual emissions for each source from the divergence field (Beirle et al., 2019; de Foy and Schauer, 2022; Goldberg et al., 2022). The PHLET method estimates NO_x emissions at a high resolution of $0.05^\circ \times 0.05^\circ$ using the adjoint method. It assumes that the NO₂ TVCDs remain in a steady-state for a period, considering the influence of local nonlinear chemistry on transport and lifetime (Kong et al., 2019).

3.2 Co-emitted CO₂ and NO_x from combustion sources

During fossil fuel combustion, CO₂ and NO_x exhibit co-emission characteristics temporally and spatially (Fig. 2). CO₂ is generated from the combustion of fossil fuels, while NO_x arises from the oxidation of nitrogen within the fuel and the decomposition of atmospheric N₂ at elevated temperatures including thermal, prompt, and fuel NO_x (Correa, 1993; Graven et al., 2009). This congruence in emission processes inspires a concept and presents an opportunity to advance the simultaneous control of greenhouse gases and air pollutants, thereby addressing the dual challenge of climate change mitigation and air quality improvement (Shi et al., 2022). The co-inversion and co-monitoring of NO_x and FFCO₂ emissions are not only feasible but also imperative.

The CO₂-to-NO_x emission ratios (ERs) vary substantially across different source sectors. Thermal power

generation, characterized by high coal consumption and the implementation of flue gas denitrification technologies, tends to have the highest ERs. The transport sector, predominantly reliant on oil consumption, has the lowest ERs (Zheng et al., 2018; Zhao et al., 2024). These ERs are influenced by factors including fuel characteristics, oxidation ratio, operating condition, and post-treatment device (Ammoura et al., 2014; Silva and Arellano, 2017; Bares et al., 2018; Fu et al., 2022). CO₂ emission factors differ markedly across fuel types, declining from coal (97.3–96.8 gCO₂/MJ) to oil (59.1–73.9 gCO₂/MJ), and natural gas (50 gCO₂/MJ) (IPCC, 2006). NO_x emission factors from combustion processes are more influenced by temperature and post-treatment technologies, which vary by source. For instance, in thermal power plants, NO_x emissions

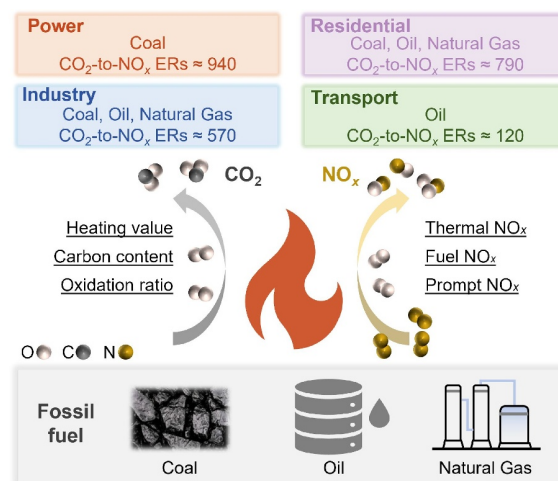


Fig. 2 Co-emission characteristics of CO₂ and NO_x during fossil fuel combustion. Note that the sectoral CO₂-to-NO_x emission ratios (ERs) are for China in 2019 derived from the Multi-resolution Emission Inventory for China (MEIC).

increase with temperature due to the contribution of thermal NO_x (Thompson et al., 1972; Abel et al., 2017). In the transport sector, diesel-powered vehicles emit more NO_x at lower ambient temperatures due to the decreased efficiency of post-combustion NO_x control technologies in cold conditions (Grange et al., 2019). Higher CO_2 -to- NO_x ERs generally indicate stricter emission controls and improved oxidation ratios (Lei et al., 2022), and they can serve as indicators of national economic development (Miyazaki and Bowman, 2023).

The complexities associated with CO_2 -to- NO_x ERs pose challenges in data acquisition. Direct *in situ* measurement of CO_2 and NO_x emissions across all processes is impractical due to the time-consuming and labor-intensive nature of the task. Recent advancements in remote sensing satellites have enabled the use of observed CO_2 and NO_2 concentrations (mostly space-borne monitor) as a novel approach to characterize oxidation ratios or emission properties for point sources and broader scales (Reuter et al., 2014; Silva and Arellano, 2017; Park et al., 2021). Ammoura et al. (2014) employed *in situ* monitored CO_2 and NO_2 concentration ratios to characterize their co-emission from traffic in a tunnel study. Lindenmaier et al. (2014) utilized multiscale CO_2 and NO_2 concentrations to differentiate emission factors from two coal-fired power plants with varying scrubbing technologies. MacDonald et al. (2023) analyzed the enhancement ratios of $\text{OCO}-2$ CO_2 and TROPOMI NO_2 concentrations in 27 large urban areas worldwide, utilizing this data to identify potential biases contributing to discrepancies between observations and inventories.

3.3 Framework inferring CO_2 emissions from NO_2 retrievals

The co-emission characteristics of FFCO_2 and NO_x has sparked the growing research interest in introducing NO_2 as a proxy to infer FFCO_2 emissions with several advantages. NO_2 anomalies induced by emission sources are more distinguishable from the background compared to CO_2 anomalies, showing magnitudes higher (Hakkarainen et al., 2016; Liu et al., 2024). The short atmospheric lifetime of NO_2 , lasting several hours, renders its concentration highly responsive to emission sources and their changes (Lange et al., 2022; Li et al., 2023a). Conversely, CO_2 possesses a much longer lifetime of hundreds of years (Eby et al., 2009), resulting in a high background concentration (hundreds of ppm) and only a marginal increase of several ppm due to proximate emission sources (Nassar et al., 2017; Reuter et al., 2019). Consequently, the response of CO_2

concentration to local and regional anthropogenic emissions is insensitive (Chevallier et al., 2020). Furthermore, NO_2 predominantly originates from anthropogenic sources, whereas CO_2 stems from both anthropogenic and biogenic sources (Ciais et al., 2014; Zheng et al., 2023). This makes NO_2 a valuable proxy for disentangling anthropogenic CO_2 emissions. Study indicates that approximately 92% of CO_2 emissions can be detected through satellite NO_2 plumes, highlighting the potential of NO_2 as an effective proxy for FFCO_2 emissions (Finch et al., 2022).

There are two primary methodologies for integrating satellite NO_2 data into CO_2 emission estimation (Fig. 3). For the first method, researchers utilize NO_2 observations as locators, constraints, or validators for deciphering CO_2 emission plumes. Satellite NO_2 column observations serve to pinpoint fossil fuel emission sources and provide constraints on plume shapes for CO_2 plume analysis (Fujinawa et al., 2021; Fuentes Andrade et al., 2024). By initially detecting and determining the plume shape with easily monitored NO_2 , this approach avoids the need for extensive scanning of the CO_2 swath, which has a low signal-to-noise ratio, thereby enhancing computational accuracy and efficiency (Reuter et al., 2019). Likewise, NO_2 observations can serve as validators for evaluating CO_2 enhancements resulting from nearby sources (Kiel et al., 2021).

For the second method, studies employ the ERs-based inversion approaches, wherein NO_2 observation-constrained NO_x emissions are first estimated. These NO_x emissions are subsequently converted to CO_2 emissions using CO_2 -to- NO_x ERs. A crucial component in the first step involves establishing the relationship between NO_2 concentration and NO_x emissions, which can be achieved through various approaches (detailed discussion in Section 3.1). For instance, Berezin et al. (2013) utilized the trend of GOME and SCIAMACHY NO_2 column data to derive long-term NO_x emission trends from 1996 to 2008 based on an assumed linear relationship. Zheng et al. (2020b) calculated the grid-by-grid responses of NO_2 concentration changes to NO_x emission variations by introducing a 40% emission perturbation in GEOS-Chem simulations. Zhang et al. (2023) employed a superposition column model to fit the TROPOMI NO_2 line density over a domain to estimate daily NO_x emissions.

Obtaining CO_2 -to- NO_x ERs is relatively challenging, with most studies directly adopting regional emission ratios from existing inventories, such as the Regional Emission Inventory in Asia (REAS) (Berezin et al., 2013), the continuous emissions monitoring system (CEMS) (Liu et al., 2020), and the Air Benefit and

Attainment and Cost Assessment System Emission Inventory (ABACAS) (Zhang et al., 2023). Efforts are underway to improve these ratios. Some studies have attempted to use observed CO₂-to-NO₂ concentration ratios as reported ERs constraints, assuming that observed atmospheric enhancement ratios partly reflect the ERs (Reuter et al., 2014; Wren et al., 2023). Additionally, Zheng et al. (2020b) dynamically updated sectoral ERs at a daily and grid-scale based on the Multi-resolution Emission Inventory for China (MEIC), considering the spatiotemporal variations in sectoral contribution to emissions.

3.4 Application spanning from point source to country

The integration of NO₂ into CO₂ emission inversion methods has been widely applied across various spatial scales, ranging from point sources and urban regions to national levels. At the point sources level, researchers typically employ plume-based methods to estimate CO₂ emissions from power and industrial facilities (Kononov et al., 2016; Fujinawa et al., 2021). Notably, Reuter et al. (2019) utilized co-located NO₂ observations from TROPOMI to constrain the shape of CO₂ plumes observed by OCO-2, enabling the calculation of cross-sectional fluxes and CO₂ emissions for 6 hotspot areas. Liu et al. (2020) estimated CO₂ emissions from 21 individual power plants by integrating EMG-updated NO_x emissions and CO₂-to-NO_x ERs. Additionally, Hakkarainen et al. (2023) applied the CSF method to estimate CO₂ emissions from 6 power plants based on OCO-3 CO₂ plumes, leveraging TROPOMI NO₂ data for shape constraints. It is noteworthy that with the rapid development of computing power, deep learning algorithms, such as CNN, are being used to calculate local CO₂ emissions from satellite images (Dumont Le Brazidec et al., 2024).

At the city scale, researchers begin by estimating NO_x emissions using the plume method before converting them to CO₂ emissions based on the reported ERs. Goldberg et al. (2019a) utilized the EMG method to update NO_x emissions for 8 cities using OMI observations, subsequently converting them to CO₂ emissions with CO₂-to-NO_x ERs from inventories provided by the US Environmental Protection Agency. Zhang et al. (2023) improved the superposition column model to estimate daily NO_x emissions in Wuhan, utilizing reported CO₂-to-NO_x ERs for CO₂ emission estimation. The MB method applies to city-scale emission inversion, as well. Yang et al. (2023) established empirical relationships between OCO-3 CO₂ SAM and TROPOMI NO₂ in three urban cities, applying

these relationships to NO₂ fields to infer NO₂-derived CO₂ fields for CO₂ emission estimation using a simplified mass balance approach.

At the national level, the ERs-based inversion approaches are prevalent. Berezin et al. (2013) quantified multiannual changes in FFCO₂ emissions from China using GOME and SCIAMACHY NO₂ retrievals in conjunction with ERs from inventories. In an early application of data assimilation, Kononov et al. (2016) optimized NO_x emissions in Europe by minimizing the bias between modeled and observed NO₂ column concentrations, subsequently converting them to CO₂ emissions based on reported ERs. Zheng et al. (2020b) and Li et al. (2023b) integrated satellite constraints and inventory sectoral profiles to infer sectoral NO_x emissions using the MB method, further translating them into sectoral CO₂ emissions in China. Miyazaki and Bowman (2023) employed a state augmentation technique (a kind of data assimilation), to infer NO_x emissions first, then converted them to CO₂ emissions over multiple countries using reported ERs. Feng et al. (2024) utilized a data assimilation system (RAPAS) to deduce NO_x emissions and thereafter projected CO₂ emissions, with surface observation of NO₂ concentrations.

4 Structural and data uncertainties

4.1 Structural uncertainties and impacts

Considerable progress has been made in estimating CO₂ emissions using NO₂ as a proxy, yet several structural uncertainties remain (Fig. 4). Establishing the relationship between atmospheric species concentration and emissions is fundamental to all inversion frameworks, which also represents the primary source of uncertainty. Current methodologies inherently involve certain assumptions. For example, plume-based methods presuppose that the shapes and spatial coverage of CO₂ and NO₂ plumes are similar or even identical (Reuter et al., 2019). However, this assumption does not always hold due to their different chemical reactivity and diffusion characteristics (Massman, 1998; Squadrito and Pryor, 1998). Another assumption is that the distribution of concentrations (e.g., plume) reflects the magnitude of emissions nearby as an aggregated source. This assumption is highly sensitive to wind fields and the spatial coverage of the plume (Kim et al., 2020a; Kurchaba et al., 2024), while not applicable at larger scales like region or country. In the case of the ERs-

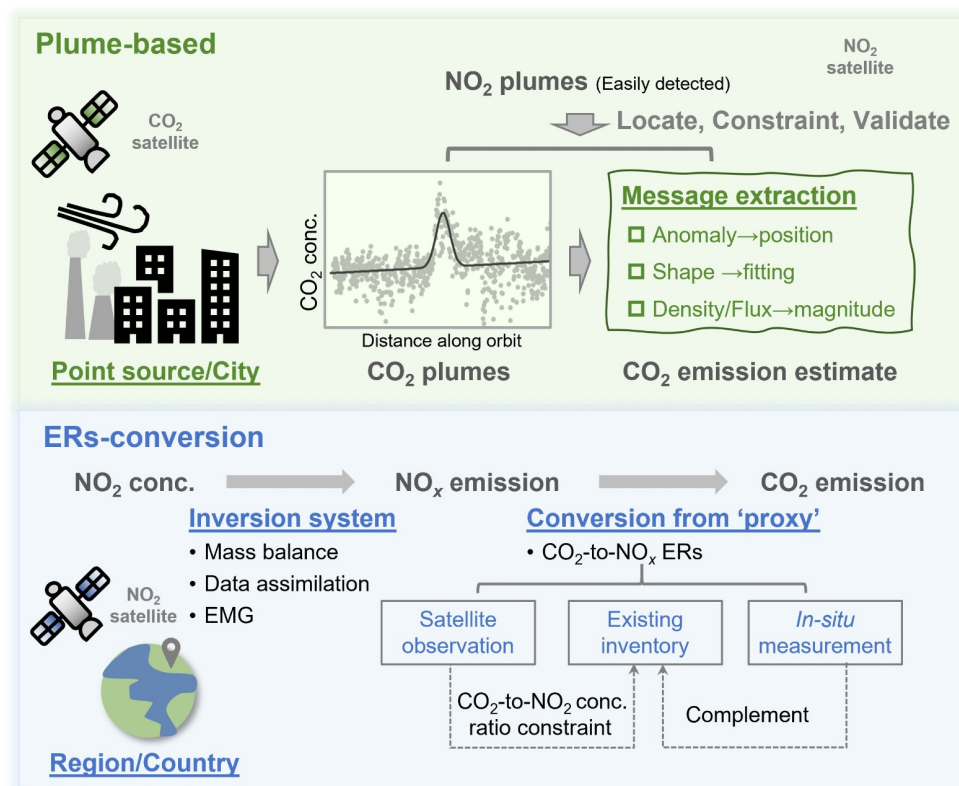


Fig. 3 Two categories of NO₂-based CO₂ emission estimate methods.

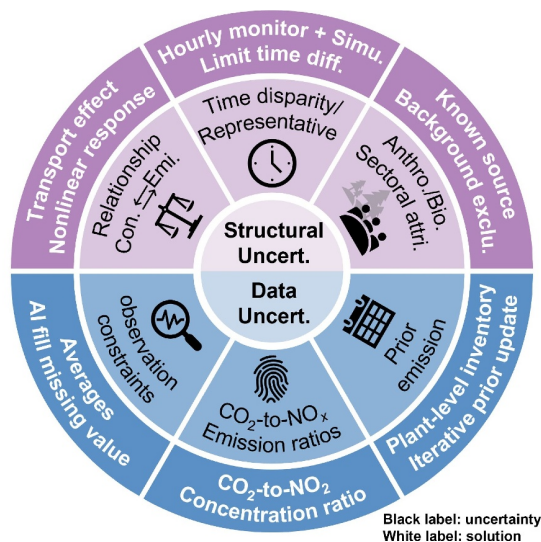


Fig. 4 Uncertainties in NO₂-based CO₂ emission inversion (black labels in the inner ring) and possible solutions (white labels in the outer ring).

based inversion approaches, the uncertainty sources vary according to their underlying principles. For instance, CTM-associated inversions are subject to systematic errors intrinsic to the physical and chemical

mechanism inside CTM (Shah et al., 2023), while MB methods are affected by the ‘smearing effect’ due to horizontal transport of the species (Palmer et al., 2003). Although eliminating biases in the relationship between concentration and emissions is rather challenging, researchers have employed various strategies to approximate this relationship, such as using relative changes to reduce the systematic errors’ impact.

Satellite remote sensing, typically aboard polar-orbiting satellites and used as observational constraints, samples only at specific times of the day. For example, TROPOMI provides global daily NO₂ column concentrations with a local time of approximately 13:30 (van Geffen et al., 2022), while OCO-3 monitors CO₂ at varying local overpass times (Taylor et al., 2023). Current studies utilizing the ERs-based inversion approaches generally rely on concentrations at a specific moment or averaged over a period to represent average concentrations. However, NO₂ and CO₂ column concentrations typically decrease around noon and peak at night (Olsen and Randerson, 2004; Li et al., 2021), while the FFCO₂ emissions peak around noon but decline at night (Nassar et al., 2013). This asynchrony in their diurnal variation weakens the temporal representativeness of remote sensing data. To

tackle this issue, some studies combine hourly-monitored concentrations with CTM simulations to restore diurnal changes in remote sensing data (Boersma et al., 2009). Another challenge arises when jointly using multiple satellites, such as OCO-3 and TROPOMI, where the research assumes that the captured plumes are temporally consistent. However, the sampling times of different satellites often do not align. Consequently, this assumption leads to data incompatibility issues, particularly in the plume-based methods (Hakkarainen et al., 2023). To mitigate this time incompatibility, researchers try to limit the time difference within a certain range when incorporating different satellite data for usage.

Distinguishing anthropogenic emissions from biogenic sources and attributing them to specific sectors remains challenging given the mixed nature of all sourced NO₂ or CO₂ concentrations in the atmosphere. The plume-based method is susceptible to natural flux fluctuations (Attermeyer et al., 2021), while the sectoral attribution of anthropogenic emissions through the ERs-based inversion approaches is challenging (Qu et al., 2022). Although NO₂ aids in disentangling anthropogenic emissions, the impact of biogenic sources, such as soil emissions, becomes noticeable in summer (Lu et al., 2021). Currently, the plume-based methods are mainly conducted near known emission sources, and studies with the ERs-based inversion approaches usually exclude natural backgrounds by setting a concentration threshold, or exclusively perturbing anthropogenic emissions while fixing biogenic sources. However, neither approach can reliably estimate FFCO₂ emissions in any industrialized region. Future advancements in finer and more accurate emission inventory compilation and satellite observation technology are expected to enhance source identification and attribution.

4.2 Data uncertainties and management

The uncertainty of observational constraints, particularly those from remote sensing, ranks foremost among data uncertainties in inversion methods. Satellite monitoring translates spectral signals into concentrations, a process sensitive to retrieval parameters including viewing geometry, cloud fraction, aerosol presence, surface albedo, and snow content (Lin et al., 2014; Lamsal et al., 2021). Additionally, the spatiotemporal coverage provided by satellites is often insufficient for emission inversion on a daily scale or fine spatial resolution (e.g., kilometer level). These retrieval errors, especially random ones, and poor coverage can be mitigated by using averaged data over extended periods.

For instance, Beirle et al. (2023) targeted point sources by calculating the divergence of NO₂ flux averaged over three years. AI approaches have also proven effective in filling in missing satellite retrieval data (Wei et al., 2022).

The CO₂-to-NO_x ERs are key parameters in the ERs-based inversion approaches, which are primarily derived from available emission inventories. Therefore, the accuracy and timeliness of converted CO₂ emissions are highly contingent on the inventory, whose emission factors are mainly derived from widely adopted references (e.g., IPCC guidelines) or empirical extrapolation. Kononov et al. (2016) demonstrated that different ERs settings could result in emission biases of up to 24.9%, comparable to or even larger than the uncertainty of emission inventory (Solazzo et al., 2021). Currently, comprehensive industry-wide emission factors are still lacking, despite efforts to measure in situ sector-specific emission factors (Park et al., 2011; Shen et al., 2014). Moreover, ERs can vary over time due to changes in emission controls, energy structures, and sectoral contributions (Luderer et al., 2022; Li et al., 2023c). As obtaining comprehensive in situ measured data are impractical, researchers continue to optimize CO₂-to-NO_x ERs given their critical role in CO₂ conversion. For example, simultaneous monitoring of CO₂ and NO₂ concentrations has been used as constraints of ERs (Wren et al., 2023). Future advancements in satellite technology capable of simultaneously monitoring NO₂ and CO₂ will further strengthen these constraints.

Most inversion methods rely on a specific prior, usually a bottom-up inventory, serving as the base for posterior emission updates. However, compiling bottom-up inventories introduces uncertainties stemming from activity data and emission factors (Solazzo et al., 2021). The mapping of emission inventory with spatial proxies introduces additional uncertainties in emissions due to their spatial mismatch (Zheng et al., 2017). These uncertainties can propagate into the NO₂-based CO₂ emission inversion process. In the plume-based methods, the prior acts as an anchor for emission attribution, implying that uncertainty in the emission location within the prior can lead to misinterpretation of emission estimates. In contrast, in the ERs-based inversion approaches, the prior establishes a baseline that influences the posterior estimates by introducing inaccurate ERs (Solazzo et al., 2021). Data assimilation requires grid-level uncertainty (Choulga et al., 2021), yet most inventories only report uncertainty ranges for total emission estimates. Efforts have been made to optimize priors and develop more accurate inventories. For instance, Cooper et al. (2017)

and Li et al. (2019) iteratively updated priors for subsequent posteriors in conventional MB methods, resulting in notable improvements. Researchers are also working on establishing plant-specific emission inventories (Lei et al., 2023; Xu et al., 2023). With the development of multisource data fusion, developing accurate and timely updated inventories is becoming increasingly feasible, thereby reducing the uncertainties associated with their use as priors.

5 Emerging trends and future avenues

5.1 Next-generation satellites

The aforementioned uncertainties have proposed several requirements for the next-generation satellites (Fig. 5). These satellites are expected to possess several improved capabilities, including simultaneous monitoring of CO₂ and NO₂ concentration, hourly remote sensing, high signal-to-noise ratios and spatial resolution, and wide swath coverage. The co-monitoring of multiple species addresses spatiotemporal discrepancies in joint satellite usage, offering better mutual verification and constraints for ERs (Bernd et al., 2021). Hourly observations, such as those from geostationary satellites, capture diurnal profiles, addressing the insufficient representativeness of specific time sampling (Penn and Holloway, 2020). High signal-to-noise ratios and spatial resolution enable finer mapping of concentrations, facilitating the identification of emission-induced enhancements from background levels (Broquet et al., 2018). Wide swath capabilities extend spatial coverage to encompass both emission sources and background areas, allowing for the capture of entire plumes (Pillai et al., 2016).

While achieving high spatial and temporal resolutions simultaneously with satellites seems unlikely at present, several upcoming satellites are equipped with some of these characteristics. For instance, the ESA and the European Commission have committed to launching a CO₂ satellite imagery, the CO2M, in 2026. This satellite will monitor atmospheric CO₂ and NO₂ concentrations at a high spatial resolution (4 km × 4 km) along a 250 km wide swath and achieve global coverage within 5 days (Bernd et al., 2019). GHGSat, a company specializing in commercial greenhouse gas satellites (Jervis et al., 2021), launched GHGSat-C10 in 2023, which is capable of detecting individual CO₂ sources with a resolution of up to 25 m, such as refineries, steel mills, and cement plants. Likewise,

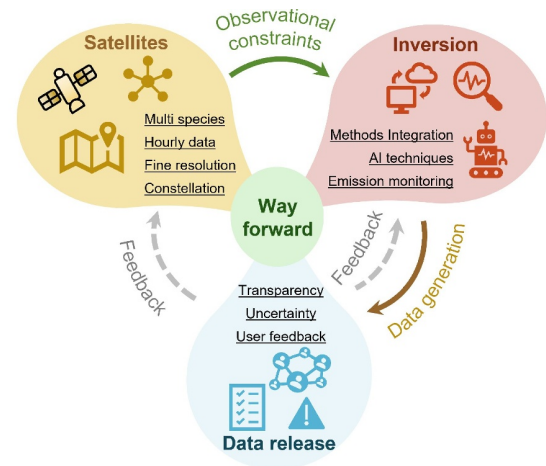


Fig. 5 Future perspectives of NO₂-based CO₂ emission inversion method.

advancements in NO₂ satellite technology are promising, particularly with geostationary satellites. TEMPO, launched in 2023, can provide hourly observational data for North America at a resolution of 2 km × 4.5 km (Zoogman et al., 2017). Additionally, the ESA plans to launch Sentinel-4 in 2024 to monitor hourly air quality across Europe (Ingmann et al., 2012). Hourly monitoring of NO₂ column concentrations enables the inversion estimate of hourly NO_x emissions, representing more accurately diurnal fluctuations in NO₂ concentrations and lifetimes. This enhanced monitoring capability improves the establishment of the concentration-emission relationship, thereby reducing uncertainties in emission inversion (Xu et al., 2024). Nevertheless, the global application of geostationary satellites is hindered by their limited coverage of specific regions. The deployment of these satellites is expected to reduce existing uncertainties in NO₂-based CO₂ emission inversion systems.

The satellites mentioned above, as well as those currently available, are passive remote sensors that measure the sunlight spectrum. Besides, active sensors first illuminate the target and then capture the reflected light. This self-emission characteristic enables them to provide high-precision data even under complex conditions. Presently, active remote sensors have been solely employed in aerosol detection (e.g., CALIPSO satellite) within atmospheric composition studies (Winker et al., 2009). Future advancements are anticipated to extend the application of active remote sensing satellites to monitor additional atmospheric components, such as NO₂ and CO₂.

Advancements have also been made in satellite constellations (Ulybyshev, 2008), which refers to a network of multiple satellites working together in space

with specific configurations and orbital arrangements to achieve global coverage, real-time monitoring, and high-resolution observation of the Earth's surface (Singh et al., 2020). Currently, constellations support research and applications in numerous fields, including global navigation, telecommunications, environmental monitoring, and natural disaster response (Maral et al., 1991; Hao et al., 2018; del Portillo et al., 2019). Several studies have investigated the optimal number of satellites required for effective global coverage in a constellation, specifically examining whether three or four satellites suffice (Zhu and Gao, 2017). Additionally, research has explored the potential of satellite constellations for CO₂ emission inversion (Lespinas et al., 2020). As satellite constellations continue to mature with wider adoption, their benefits of extensive coverage, near-real-time data retrieval, and high-resolution capabilities are expected to drive further advancements in the field of CO₂ emission inversion.

5.2 Development of new inversion methods

In addition to refining observational techniques, the development of novel inversion methods is imperative, albeit challenging. Key avenues for advancement are elucidated as follows:

1) Establishing a concentration-emission relationship at a granular level (e.g., hundred meters, point source) in tandem with the advancement of satellite technologies. Finer resolution approximates the localized relationship between concentration and emissions, aiding in the attribution to specific sources and thus targeting those with substantial potential for emission reduction. For example, incorporating inter-grid transport and nonlinear responses in the MB method can overcome resolution limitations, facilitating subsequent emission attribution (Turner et al., 2012). High resolution also benefits the capture of plumes downwind from sources and the extraction of emission magnitude therein (He et al., 2024a). Another inquiry arises: How can we precisely assess the reliability and accuracy of estimated emissions? As high-resolution emission inversion techniques continue to advance, ensuring the reliability and accuracy of estimated emissions becomes increasingly crucial. One effective approach is to refine plant-level emission monitoring (regarded as a “truth”) to verify inversion results (Tang et al., 2023). This method also provides foundational data for delineating emission reduction responsibilities and evaluating the effectiveness of emissions reduction efforts.

2) Amalgamating diverse methodologies that harbor complementary strengths to achieve spatiotemporal

refinement. Current techniques often require a trade-off between refinement across different dimensions, typically sacrificing one to enhance another. For instance, achieving high spatial resolution (kilometer scale) often necessitates a reduction in temporal resolution (monthly or annual average). These methods have independently advanced various dimensions, such as finer temporal resolution (days or even hours), spatial resolution (kilometers), and detailed sectoral attribution. The integration of strengths from various approaches can enable simultaneous multi-dimensional refinement. Moon et al. (2024) combined IFDDB and 4D-Var as a hybrid inversion system to estimate NO_x emissions in South Korea, wherein IFDDB constraining spatial distribution and 4D-Var estimating temporal variations on an hourly scale. Tibrewal et al. (2024) integrated an ensemble of bottom-up inventories and inversions from the Global Carbon Project to resolve CH₄ emissions from coal, oil, and natural gas exploitation for major producing nations. The synergistic use of multiple tools can overcome the limitations of individual methods, enabling simultaneous advancements across multiple dimensions.

3) Integrating emerging analytical paradigms, Data Science and AI, to enhance the efficiency and accuracy of processing extensive multi-source datasets. With the surge in satellite retrievals and the growing computational burden of model simulations, coupled with the demand for near-real-time inversion, conventional data processing methods are becoming inadequate. In this context, leveraging new analytical methods to improve efficiency is becoming imperative (Vance et al., 2024). Data Science plays a pivotal role in processing big data by applying advanced statistical techniques and algorithms (zu Castell et al., 2022). For instance, data fusion combines information from multiple sources, enhancing the accuracy and completeness of datasets. This method offers special advantages in NO₂-based CO₂ emission inversion due to the multi-source datasets involved, including CO₂ and NO₂ satellites, emission inventories, and model simulations. Besides, AI substantially improves efficiency and automation capabilities. Using AI to train on a subset of data allows for the extraction of effective information and internal connections within big data, which can then be quickly applied to newly generated data. A sophisticated AI can supersede manual plume identification and the modeling of concentration-emission relationships. Finch et al. (2022) utilized a CNN to automatically identify NO₂ plumes observed by TROPOMI. Joyce et al. (2023) implemented a deep neural network to effectively identify and quantify CH₄ emissions from

point sources using satellite imagery at 30 m resolution. Dumont Le Brazidec et al. (2024) demonstrated that the CNN can automatically learn to identify the XCO₂ plume and assess emissions based on the plume concentrations. Overall, the adaptability, learning, and scalability of AI techniques demonstrate strong potential for reliable and efficient big-data-based emission inversion, such as NO₂-based CO₂ emission inversion involving multiple species.

5.3 Data stewardship and sharing with caution

Despite extensive efforts and opportunities to enhance the accuracy of inferred emissions, clear and detailed caveats must accompany the released datasets to users. The compilation of a rigorous dataset for universal use necessitates publishers to include a statement of uncertainty and scope of application, similar to the IPCC report or the Product User Manual of satellite data. This attachment should provide comprehensive information to enable users to accurately interpret and utilize the dataset, thus mitigating the risk of misuse. The principles in data stewardship and sharing include transparency and clarity, delineation of application scope, uncertainty statements, provision of examples and usage recommendations, and ongoing updates and communication.

Firstly, clear and understandable documentation should be published to elucidate the data's sources, processing methodologies, and potential influencing factors. This ensures users grasp the background and limitations of the data. Secondly, defining the scope of application for the data and elucidating it in the documentation aids users in understanding their specific utility and limitations. Thirdly, accompanying data releases with uncertainty statements is crucial, detailing the data's accuracy and reliability. This may involve confidence intervals, potential biases or error ranges, and uncertainties associated with the data generation process. Incorporating attributes quantifying the data quality, such as the `quality_flag` in TROPOMI NO₂ retrievals (van Geffen et al., 2020), enhances the practicability. Fourthly, offering examples and usage recommendations assists users in correctly interpreting and utilizing the data. This could include data visualization examples, data processing advice, practices tailored to specific domains, and processing scripts. Finally, ensuring regular updates to data products and maintaining open communication channels with users to promptly address any issues or feedback fosters trust and enhances user satisfaction with the data products.

Some data stewardship and sharing have met the aforementioned standards. For instance, when KNMI released the TROPOMI L2 NO₂ satellite data product, they included comprehensive documentation such as data definitions and product user manuals. Additionally, several bottom-up inventory datasets are continuously updated post-release, maintaining user communication and improving emission data. Notable examples include the MEIC, Carbon Monitor, Emissions Database for Global Atmospheric Research (EDGAR), and the Community Emissions Data System (CEDS). Due to their later development, inversion data currently lacks a mature framework for data stewardship and sharing. However, these frameworks can draw valuable insights from the established practices of emission inventory data.

6 Conclusions

To facilitate the attainment of NDCs, the GST has been implemented as a “ratchet mechanism” every five years since 2023, emphasizing the necessity for establishing anthropogenic CO₂ MVS capacity, particularly FFCO₂. Research endeavors aimed at compiling more accurate, detailed, and timely FFCO₂ emission inventories are flourishing. Despite progress in direct CO₂ emission inversion based on CO₂ observations, challenges persist due to the long lifetime of atmospheric CO₂, which obscures concentration enhancements above the background. CO₂ emission inversion solely reliant on CO₂ concentration does not work for larger spatial scales, such as regional and national levels. In contrast, the short lifespan of co-emitted NO_x, with enhancements substantially higher than background levels, presents a more viable proxy. Therefore, integrating NO₂ observation has emerged as a promising strategy for CO₂ emission inversion. Two prevalent methodological systems include: 1) using NO₂ observations to locate, constrain, and validate CO₂ plumes from nearby sources, particularly for point sources (plume-based method); and 2) inferring NO_x emissions from NO₂ observations, followed by their conversion to CO₂ emissions using CO₂-to-NO_x ERs (ERs-based inversion approach), which is often applied at the national scale.

Despite the advantages of using NO₂ as a proxy for inferring FFCO₂ emissions, inherent uncertainties persist. Structural uncertainties include 1) the establishment of relationships between concentrations and emissions at fine scales; 2) the representativeness of satellite retrievals sampled at specific times; and 3) the disentanglement of anthropogenic emissions from

biogenic sources. Additionally, data uncertainties stem from satellite retrievals, CO₂-to-NO_x ERs, and priors. To date, numerous studies have been dedicated to mitigating these challenges, yet they remain formidable. Future efforts hold substantial promise, including the deployment of next-generation satellites and the development of advanced inversion systems. Achieving these objectives will necessitate collaboration among diverse research communities, including remote sensing, emission inventory, transport model improvement, and atmospheric inversion algorithm development. This interdisciplinary cooperation is vital for enhancing the accuracy and reliability of CO₂ emission estimates, supporting the GST ratchet mechanism, and ultimately contributing to the Paris Agreement's objective of limiting global temperature rise to within 2 °C (ideally 1.5 °C).

Acknowledgements This work was supported by the National Natural Science Foundation of China (No. 42105094).

Conflict of Interests The authors declare that the research was conducted in the absence of any commercial or financial relationships that could be construed as a potential conflict of interest.

Electronic Supplementary Material Supplementary material is available in the online version of this article at <https://doi.org/10.1007/s11783-025-1922-x> and is accessible for authorized users.

Open Access This article is licensed under a Creative Commons Attribution 4.0 International License, which permits use, sharing, adaptation, distribution and reproduction in any medium or format, as long as you give appropriate credit to the original author(s) and the source, provide a link to the Creative Commons licence, and indicate if changes were made. The images or other third party material in this article are included in the article's Creative Commons licence, unless indicated otherwise in a credit line to the material. If material is not included in the article's Creative Commons licence and your intended use is not permitted by statutory regulation or exceeds the permitted use, you will need to obtain permission directly from the copyright holder. To view a copy of this licence, visit <http://creativecommons.org/licenses/by/4.0/>.

References

- Abel D, Holloway T, Kladar R M, Meier P, Ahl D, Harkey M, Patz J (2017). Response of power plant emissions to ambient temperature in the Eastern United States. *Environmental Science & Technology*, 51(10): 5838–5846
- Ammoura L, Xueref-Remy I, Gros V, Baudic A, Bonsang B, Petit J E, Perrussel O, Bonnaire N, Sciare J, Chevallier F (2014). Atmospheric measurements of ratios between CO₂ and co-emitted species from traffic: a tunnel study in the Paris megacity. *Atmospheric Chemistry and Physics*, 14(23): 12871–12882
- Attermeyer K, Casas-Ruiz J P, Fuss T, Pastor A, Cauvy-Fraunié S, Sheath D, Nydahl A C, Doretto A, Portela A P, Doyle B C, et al. (2021). Carbon dioxide fluxes increase from day to night across European streams. *Communications Earth & Environment*, 2(1): 118
- Bares R, Lin J C, Hoch S W, Baasandorj M, Mendoza D L, Fasoli B, Mitchell L, Catharine D, Stephens B B (2018). The wintertime covariation of CO₂ and criteria pollutants in an urban valley of the Western United States. *Journal of Geophysical Research. Atmospheres*, 123(5): 2684–2703
- Beirle S, Boersma K F, Platt U, Lawrence M G, Wagner T (2011). Megacity emissions and lifetimes of nitrogen oxides probed from space. *Science*, 333(6050): 1737–1739
- Beirle S, Borger C, Dörner S, Li A, Hu Z, Liu F, Wang Y, Wagner T (2019). Pinpointing nitrogen oxide emissions from space. *Science Advances*, 5(11): eaax9800
- Beirle S, Borger C, Jost A, Wagner T (2023). Improved catalog of NO_x point source emissions (version 2). *Earth System Science Data*, 15(7): 3051–3073
- Berezin E V, Konovalov I B, Ciais P, Richter A, Tao S, Janssens-Maenhout G, Beekmann M, Schulze E D (2013). Multiannual changes of CO₂ emissions in China: indirect estimates derived from satellite measurements of tropospheric NO₂ columns. *Atmospheric Chemistry and Physics*, 13(18): 9415–9438
- Bernd S, Jean-Loup B Z, Armin L S, Yasjka M (2019). The European CO₂ monitoring mission: observing anthropogenic greenhouse gas emissions from space. *Proc. SPIE 11180, International Conference on Space Optics—ICSO 2018, 111800M* (12 July 2019, Chania, Greece)
- Bernd S, Valerie F, Bézy J L, Meijer Y, Durand Y, Courrèges-Lacoste G B, Pachot C, Löscher A, Nett H, Minoglou K, et al. (2021). The Copernicus CO₂M mission for monitoring anthropogenic carbon dioxide emissions from space. *Proc. SPIE 11852, International Conference on Space Optics — ICSO 2020, 118523M* (11 June 2021, Online Only)
- Boersma K F, Jacob D J, Trainic M, Rudich Y, Desmedt I, Dirksen R, Eskes H J (2009). Validation of urban NO₂ concentrations and their diurnal and seasonal variations observed from the SCIAMACHY and OMI sensors using *in situ* surface measurements in Israeli cities. *Atmospheric Chemistry and Physics*, 9(12): 3867–3879
- Bovensmann H, Buchwitz M, Burrows J P, Reuter M, Krings T, Gerilowski K, Schneising O, Heymann J, Tretnier A, Erzinger J (2010). A remote sensing technique for global monitoring of power plant CO₂ emissions from space and related applications. *Atmospheric Measurement Techniques*, 3(4): 781–811
- Bovensmann H, Burrows J P, Buchwitz M, Frerick J, Noël S, Rozanov V V, Chance K V, Goede A P H (1999). SCIAMACHY: mission objectives and measurement modes. *Journal of the Atmospheric Sciences*, 56(2): 127–150
- Broquet G, Bréon F M, Renault E, Buchwitz M, Reuter M, Bovensmann H, Chevallier F, Wu L, Ciais P (2018). The potential of satellite spectro-imagery for monitoring CO₂ emissions from large cities. *Atmospheric Measurement Techniques*, 11(2): 681–708

- Buchwitz M, Reuter M, Noël S, Bramstedt K, Schneising O, Hilker M, Fuentes Andrade B, Bovensmann H, Burrows J P, Di Noia A, et al. (2021). Can a regional-scale reduction of atmospheric CO₂ during the COVID-19 pandemic be detected from space? A case study for East China using satellite XCO₂ retrievals. *Atmospheric Measurement Techniques*, 14(3): 2141–2166
- Burrows J P, Hölzle E, Goede A P H, Visser H, Fricke W (1995). SCIAMACHY: scanning imaging absorption spectrometer for atmospheric chartography. *Acta Astronautica*, 35(7): 445–451
- Burrows J P, Weber M, Buchwitz M, Rozanov V, Ladstätter-Weissenmayer A, Richter A, Debeek R, Hoogen R, Bramstedt K, Eichmann K U, et al. (1999). The global ozone monitoring experiment (GOME): mission concept and first scientific results. *Journal of the Atmospheric Sciences*, 56(2): 151–175
- Byrne B, Baker D F, Basu S, Bertolacci M, Bowman K W, Carroll D, Chatterjee A, Chevallier F, Ciais P, Cressie N, et al. (2023). National CO₂ budgets (2015–2020) inferred from atmospheric CO₂ observations in support of the global stocktake. *Earth System Science Data*, 15(2): 963–1004
- Chatterjee A, Gierach M M, Sutton A J, Feely R A, Crisp D, Eldering A, Gunson M R, O'Dell C W, Stephens B B, Schimel D S (2017). Influence of El Niño on atmospheric CO₂ over the tropical Pacific Ocean: findings from NASA's OCO-2 mission. *Science*, 358(6360): eaam5776
- Chevallier F, Broquet G, Zheng B, Ciais P, Eldering A (2022). Large CO₂ emitters as seen from satellite: comparison to a gridded global emission inventory. *Geophysical Research Letters*, 49(5): e2021GL097540
- Chevallier F, Zheng B, Broquet G, Ciais P, Liu Z, Davis S J, Deng Z, Wang Y, Bréon F-M, O'Dell C W (2020). Local anomalies in the column-averaged dry air mole fractions of carbon dioxide across the globe during the first months of the coronavirus recession. *Geophysical Research Letters*, 47(22): e2020GL090244
- Choulga M, Janssens-Maenhout G, Super I, Solazzo E, Agustí-Panareda A, Balsamo G, Bousseres N, Crippa M, Denier Van Der Gon H, Engelen R, et al. (2021). Global anthropogenic CO₂ emissions and uncertainties as a prior for Earth system modelling and data assimilation. *Earth System Science Data*, 13(11): 5311–5335
- Ciais P, Dolman A J, Bombelli A, Duren R, Peregon A, Rayner P J, Miller C, Gobron N, Kinderman G, Marland G, et al. (2014). Current systematic carbon-cycle observations and the need for implementing a policy-relevant carbon observing system. *Biogeosciences*, 11(13): 3547–3602
- Cooper M, Martin R V, Padmanabhan A, Henze D K (2017). Comparing mass balance and adjoint methods for inverse modeling of nitrogen dioxide columns for global nitrogen oxide emissions. *Journal of Geophysical Research. Atmospheres*, 122(8): 4718–4734
- Cooper M J, Martin R V, Hammer M S, Levelt P F, Veefkind P, Lamsal L N, Krotkov N A, Brook J R, McLinden C A (2022). Global fine-scale changes in ambient NO₂ during COVID-19 lockdowns. *Nature*, 601(7893): 380–387
- Correa S M (1993). A Review of NO_x Formation Under Gas-Turbine Combustion Conditions. *Combustion Science and Technology*, 87(1–6): 329–362
- Crisp D, Pollock H R, Rosenberg R, Chapsky L, Lee R A M, Oyafuso F A, Frankenberg C, O'Dell C W, Bruegge C J, Doran G B, et al. (2017). The on-orbit performance of the Orbiting Carbon Observatory-2 (OCO-2) instrument and its radiometrically calibrated products. *Atmospheric Measurement Techniques*, 10(1): 59–81
- Cusworth D H, Thorpe A K, Miller C E, Ayasse A K, Jiorle R, Duren R M, Nassar R, Mastrogiacomo J P, Nelson R R (2023). Two years of satellite-based carbon dioxide emission quantification at the world's largest coal-fired power plants. *Atmospheric Chemistry and Physics*, 23(22): 14577–14591
- de Foy B, Schauer J J (2022). An improved understanding of NO_x emissions in South Asian megacities using TROPOMI NO₂ retrievals. *Environmental Research Letters*, 17(2): 024006
- del Portillo I, Cameron B G, Crawley E F (2019). A technical comparison of three low earth orbit satellite constellation systems to provide global broadband. *Acta Astronautica*, 159: 123–135
- Dumont Le Brazidec J, Vanderbecken P, Farchi A, Bocquet M, Lian J, Broquet G, Kuhlmann G, Danjou A, Lauvaux T (2023). Segmentation of XCO₂ images with deep learning: application to synthetic plumes from cities and power plants. *Geoscientific Model Development*, 16(13): 3997–4016
- Dumont Le Brazidec J, Vanderbecken P, Farchi A, Broquet G, Kuhlmann G, Bocquet M (2024). Deep learning applied to CO₂ power plant emissions quantification using simulated satellite images. *Geoscientific Model Development*, 17(5): 1995–2014
- Eby M, Zickfeld K, Montenegro A, Archer D, Meissner K J, Weaver A J (2009). Lifetime of anthropogenic climate change: millennial time scales of potential CO₂ and surface temperature perturbations. *Journal of Climate*, 22(10): 2501–2511
- Editorial (2023). Global stocktake and beyond. *Nature Climate Change*, 13(10): 999
- Eduardo Calvo Buendia S G, Limmeechokchai B, Pipatti R, Rojas Y, Sturgiss R, Tanabe K, Wirth T, Romano D J W, Garg A, Weitz M M, et al. (2019). 2019 Refinement to the 2006 IPCC Guidelines for National Greenhouse Gas Inventories_Overview. Genève: The Intergovernmental Panel on Climate Change
- Eldering A, Taylor T E, O'Dell C W, Pavlick R (2019). The OCO-3 mission: measurement objectives and expected performance based on 1 year of simulated data. *Atmospheric Measurement Techniques*, 12(4): 2341–2370
- Eldering A, Wennberg P O, Crisp D, Schimel D S, Gunson M R, Chatterjee A, Liu J, Schwandner F M, Sun Y, O'Dell C W, et al. (2017). The Orbiting Carbon Observatory-2 early science investigations of regional carbon dioxide fluxes. *Science*, 358(6360): eaam5745
- European C, Ciais P, Palmer P, Scholze M, Kentarchos A, Brunhes T, Dolman H, Husband R, Holmlund K, Engelen R, et al. (2017). An Operational Anthropogenic CO₂ Emissions Monitoring &

- Verification System: Baseline Requirements, Model Components and Functional Architecture. Brussels: Publications Office of the European Union
- Feng S, Jiang F, Wang H, Liu Y, He W, Wang H, Shen Y, Zhang L, Jia M, Ju W, Chen J M (2024). China's fossil fuel CO₂ emissions estimated using surface observations of coemitted NO₂. *Environmental Science & Technology*, 58(19): 8299–8312
- Finch D P, Palmer P I, Zhang T (2022). Automated detection of atmospheric NO₂ plumes from satellite data: a tool to help infer anthropogenic combustion emissions. *Atmospheric Measurement Techniques*, 15(3): 721–733
- Friedlingstein P, O'sullivan M, Jones M W, Andrew R M, Bakker D C E, Hauck J, Landschützer P, Le Quéré C, Luijkx I T, Peters G P, et al. (2023). Global Carbon Budget 2023. *Earth System Science Data*, 15(12): 5301–5369
- Fu Y, Sun W, Fan D, Zhang Z, Hao Y (2022). An assessment of China's industrial emission characteristics using satellite observations of XCO₂, SO₂, and NO₂. *Atmospheric Pollution Research*, 13(8): 101486
- Fuentes Andrade B, Buchwitz M, Reuter M, Bovensmann H, Richter A, Boesch H, Burrows J P (2024). A method for estimating localized CO₂ emissions from co-located satellite XCO₂ and NO₂ images. *Atmospheric Measurement Techniques*, 17(3): 1145–1173
- Fujinawa T, Kuze A, Suto H, Shiomi K, Kanaya Y, Kawashima T, Kataoka F, Mori S, Eskes H, Tanimoto H (2021). First concurrent observations of NO₂ and CO₂ from power plant plumes by airborne remote sensing. *Geophysical Research Letters*, 48(14): e2021GL092685
- Goldberg D L, Harkey M, de Foy B, Judd L, Johnson J, Yarwood G, Holloway T (2022). Evaluating NO_x emissions and their effect on O₃ production in Texas using TROPOMI NO₂ and HCHO. *Atmospheric Chemistry and Physics*, 22(16): 10875–10900
- Goldberg D L, Lu Z, Oda T, Lamsal L N, Liu F, Griffin D, McLinden C A, Krotkov N A, Duncan B N, Streets D G (2019a). Exploiting OMI NO₂ satellite observations to infer fossil-fuel CO₂ emissions from U.S. megacities. *Science of the Total Environment*, 695: 133805
- Goldberg D L, Lu Z, Streets D G, de Foy B, Griffin D, McLinden C A, Lamsal L N, Krotkov N A, Eskes H (2019b). Enhanced capabilities of TROPOMI NO₂: estimating NO_x from North American cities and power plants. *Environmental Science & Technology*, 53(21): 12594–12601
- Grange S K, Farren N J, Vaughan A R, Rose R A, Carslaw D C (2019). Strong temperature dependence for light-duty diesel vehicle NO_x emissions. *Environmental Science & Technology*, 53(11): 6587–6596
- Graven H D, Stephens B B, Guilderson T P, Campos T L, Schimel D S, Campbell J E, Keeling R F (2009). Vertical profiles of biospheric and fossil fuel-derived CO₂ and fossil fuel CO₂: CO ratios from airborne measurements of $\Delta^{14}\text{C}$, CO₂ and CO above Colorado, USA. *Tellus B: Chemical and Physical Meteorology*, 61: 536–546
- Gu D, Wang Y, Smeltzer C, Boersma K F (2014). Anthropogenic emissions of NO_x over China: reconciling the difference of inverse modeling results using GOME-2 and OMI measurements. *Journal of Geophysical Research, D, Atmospheres*, 119(12): 7732–7740
- Hakkarainen J, Ialongo I, Koene E, Szeląg M E, Tamminen J, Kuhlmann G, Brunner D (2022). Analyzing local carbon dioxide and nitrogen oxide emissions from space using the divergence method: an application to the synthetic SMARTCARB dataset. *Frontiers in Remote Sensing*, 3
- Hakkarainen J, Ialongo I, Oda T, Szeląg M E, O'Dell C W, Eldering A, Crisp D (2023). Building a bridge: characterizing major anthropogenic point sources in the South African Highveld region using OCO-3 carbon dioxide snapshot area maps and Sentinel-5P/TROPOMI nitrogen dioxide columns. *Environmental Research Letters*, 18(3): 035003
- Hakkarainen J, Ialongo I, Tamminen J (2016). Direct space-based observations of anthropogenic CO₂ emission areas from OCO-2. *Geophysical Research Letters*, 43(21): 11400–11406
- Hao M, Zhang J, Niu R, Deng C, Liang H (2018). Application of BeiDou navigation satellite system in emergency rescue of natural hazards: a case study for field geological survey of Qinghai–Tibet plateau. *Geo-Spatial Information Science*, 21(4): 294–301
- Hassinen S, Balis D, Bauer H, Begoin M, Delcloo A, Eleftheratos K, Gimeno Garcia S, Granville J, Grossi M, Hao N, et al. (2016). Overview of the O3M SAF GOME-2 operational atmospheric composition and UV radiation data products and data availability. *Atmospheric Measurement Techniques*, 9(2): 383–407
- He C, Lu X, Zhang Y, Liu Z, Jiang F, Sun Y, Gao M, Liu Y, Lin H, Yang J, Lin X, Wang Y, Hu C, Fan S (2024a). Revisiting the quantification of power plant CO₂ emissions in the United States and China from satellite: a comparative study using three top-down approaches. *Remote Sensing of Environment*, 308: 114192
- He Z, Gao L, Liang M, Zeng Z C (2024b). A survey of methane point source emissions from coal mines in Shanxi province of China using AHSI on board Gaofen-5B. *Atmospheric Measurement Techniques*, 17(9): 2937–2956
- Hersbach H, Bell B, Berrisford P, Hirahara S, Horányi A, Muñoz-Sabater J, Nicolas J, Peubey C, Radu R, Schepers D, et al. (2020). The ERA5 global reanalysis. *Quarterly Journal of the Royal Meteorological Society*, 146(730): 1999–2049
- Heymann J, Reuter M, Buchwitz M, Schneising O, Bovensmann H, Burrows J P, Massart S, Kaiser J W, Crisp D (2017). CO₂ emission of Indonesian fires in 2015 estimated from satellite-derived atmospheric CO₂ concentrations. *Geophysical Research Letters*, 44(3): 1537–1544
- Hong X, Zhang C, Tian Y, Zhu Y, Hao Y, Liu C (2024). First TanSat CO₂ retrieval over land and ocean using both nadir and glint spectroscopy. *Remote Sensing of Environment*, 304: 114053
- Hong X, Zhang P, Bi Y, Liu C, Sun Y, Wang W, Chen Z, Yin H, Zhang C, Tian Y, Liu J (2022). Retrieval of Global carbon

- dioxide from tansat satellite and comprehensive validation with TCCON measurements and satellite observations. *IEEE Transactions on Geoscience and Remote Sensing*, 60: 1–16
- Ingmann P, Veihelmann B, Langen J, Lamarre D, Stark H, Courrèges-Lacoste G B (2012). Requirements for the GMES Atmosphere Service and ESA's implementation concept: sentinels-4/-5 and -5p. *Remote Sensing of Environment*, 120: 58–69
- IPCC (2006). 2006 IPCC Guidelines for National Greenhouse Gas Inventories: Volume I General Guidance and Reporting. Genève: The Intergovernmental Panel on Climate Change
- Jervis D, McKeever J, Durak B O A, Sloan J J, Gains D, Varon D J, Ramier A, Strupler M, Tarrant E (2021). The GHGSat-D imaging spectrometer. *Atmospheric Measurement Techniques*, 14(3): 2127–2140
- Jones M W, Peters G P, Gasser T, Andrew R M, Schwingshackl C, Gütschow J, Houghton R A, Friedlingstein P, Pongratz J, Le Quéré C (2023). National contributions to climate change due to historical emissions of carbon dioxide, methane, and nitrous oxide since 1850. *Scientific Data*, 10(1): 155
- Joyce P, Ruiz Villena C, Huang Y, Webb A, Gloor M, Wagner F H, Chipperfield M P, Barrio Guilló R, Wilson C, Boesch H (2023). Using a deep neural network to detect methane point sources and quantify emissions from PRISMA hyperspectral satellite images. *Atmospheric Measurement Techniques*, 16(10): 2627–2640
- Kiel M, Eldering A, Roten D D, Lin J C, Feng S, Lei R, Lauvaux T, Oda T, Roehl C M, Blavier J F, et al. (2021). Urban-focused satellite CO₂ observations from the Orbiting Carbon Observatory-3: a first look at the Los Angeles megacity. *Remote Sensing of Environment*, 258: 112314
- Kim H C, Chai T, Stein A, Kondragunta S (2020a). Inverse modeling of fire emissions constrained by smoke plume transport using HYSPLIT dispersion model and geostationary satellite observations. *Atmospheric Chemistry and Physics*, 20(17): 10259–10277
- Kim J, Jeong U, Ahn M H, Kim J H, Park R J, Lee H, Song C H, Choi Y S, Lee K H, Yoo J M, et al. (2020b). New era of air quality monitoring from space: geostationary environment monitoring spectrometer (GEMS). *Bulletin of the American Meteorological Society*, 101(1): E1–E22
- Kong H, Lin J, Zhang R, Liu M, Weng H, Ni R, Chen L, Wang J, Yan Y, Zhang Q (2019). High-resolution (0.05° × 0.05°) NO_x emissions in the Yangtze River Delta inferred from OMI. *Atmospheric Chemistry and Physics*, 19(20): 12835–12856
- Konovalov I B, Berezin E V, Ciaia P, Broquet G, Zhuravlev R V, Janssens-Maenhout G (2016). Estimation of fossil-fuel CO₂ emissions using satellite measurements of “proxy” species. *Atmospheric Chemistry and Physics*, 16(21): 13509–13540
- Kort E A, Frankenberg C, Miller C E, Oda T (2012). Space-based observations of megacity carbon dioxide. *Geophysical Research Letters*, 39(17): 2012GL052738
- Kuhlmann G, Henne S, Meijer Y, Brunner D (2021). Quantifying CO₂ emissions of power plants with CO₂ and NO₂ imaging satellites. *Frontiers in Remote Sensing*, 2
- Kurchaba S, Sokolovsky A, Van Vliet J, Verbeek F J, Veenman C J (2024). Sensitivity analysis for the detection of NO₂ plumes from seagoing ships using TROPOMI data. *Remote Sensing of Environment*, 304: 304
- Kuze A, Suto H, Nakajima M, Hamazaki T (2009). Thermal and near infrared sensor for carbon observation Fourier-transform spectrometer on the Greenhouse Gases Observing Satellite for greenhouse gases monitoring. *Applied Optics*, 48(35): 6716–6733
- Lamsal L N, Krotkov N A, Vasilkov A, Marchenko S, Qin W, Yang E S, Fasnacht Z, Joiner J, Choi S, Haffner D, et al. (2021). Ozone Monitoring Instrument (OMI) Aura nitrogen dioxide standard product version 4.0 with improved surface and cloud treatments. *Atmospheric Measurement Techniques*, 14(1): 455–479
- Lange K, Richter A, Burrows J P (2022). Variability of nitrogen oxide emission fluxes and lifetimes estimated from Sentinel-5P TROPOMI observations. *Atmospheric Chemistry and Physics*, 22(4): 2745–2767
- Lei R, Feng S, Danjou A, Broquet G, Wu D, Lin J C, O'Dell C W, Lauvaux T (2021). Fossil fuel CO₂ emissions over metropolitan areas from space: a multi-model analysis of OCO-2 data over Lahore, Pakistan. *Remote Sensing of Environment*, 264: 112625
- Lei R, Feng S, Xu Y, Tran S, Ramonet M, Grutter M, Garcia A, Campos-Pineda M, Lauvaux T (2022). Reconciliation of asynchronous satellite-based NO₂ and XCO₂ enhancements with mesoscale modeling over two urban landscapes. *Remote Sensing of Environment*, 281: 113241
- Lei T, Wang D, Yu X, Ma S, Zhao W, Cui C, Meng J, Tao S, Guan D (2023). Global iron and steel plant CO₂ emissions and carbon-neutrality pathways. *Nature*, 622, 514–520
- Lepinas F, Wang Y, Broquet G, Bréon F-M, Buchwitz M, Reuter M, Meijer Y, Loeschner A, Janssens-Maenhout G, Zheng B, et al. (2020). The potential of a constellation of low earth orbit satellite imagers to monitor worldwide fossil fuel CO₂ emissions from large cities and point sources. *Carbon Balance and Management*, 15(1): 18
- Levelt P F, van den Oord G H J, Dobber M R, Mäkki A, Visser H, de Vries J, Stammes P, Lundell J, Saari H. (2006). The ozone monitoring instrument. *IEEE Transactions on Geoscience and Remote Sensing*, 44(5): 1093–1101
- Li C, Martin R V, Shephard M W, Cady-Pereira K, Cooper M J, Kaiser J, Lee C J, Zhang L, Henze D K (2019). Assessing the iterative finite difference mass balance and 4D-var methods to derive ammonia emissions over North America using synthetic observations. *Journal of Geophysical Research. Atmospheres*, 124(7): 4222–4236
- Li H, Zheng B (2023a). TROPOMI NO₂ shows a fast recovery of China's economy in the first quarter of 2023. *Environmental Science & Technology Letters*, 10(8): 635–641
- Li H, Zheng B, Ciaia P, Boersma K F, Riess T C V W, Martin R V, Broquet G, Van Der A R, Li H, Hong C, et al. (2023b). Satellite reveals a steep decline in China's CO₂ emissions in early 2022.

- Science Advances, 9(29): eadg7429
- Li J, Wang Y, Zhang R, Smeltzer C, Weinheimer A, Herman J, Boersma K F, Celarier E A, Long R W, Szykman J J, et al. (2021). Comprehensive evaluations of diurnal NO₂ measurements during DISCOVER-AQ 2011: effects of resolution-dependent representation of NO_x emissions. *Atmospheric Chemistry and Physics*, 21(14): 11133–11160
- Li S, Wang S, Wu Q, Zhang Y, Ouyang D, Zheng H, Han L, Qiu X, Wen Y, Liu M, et al. (2023c). Emission trends of air pollutants and CO₂ in China from 2005 to 2021. *Earth System Science Data*, 15(6): 2279–2294
- Lin J T, Martin R V, Boersma K F, Sneep M, Stammes P, Spurr R, Wang P, Van Roozendael M, Cl  mer K, Irie H (2014). Retrieving tropospheric nitrogen dioxide from the Ozone Monitoring Instrument: effects of aerosols, surface reflectance anisotropy, and vertical profile of nitrogen dioxide. *Atmospheric Chemistry and Physics*, 14(3): 1441–1461
- Lin X, van der A R, de Laat J, Eskes H, Chevallier F, Ciais P, Deng Z, Geng Y, Song X, Ni X, et al. (2023). Monitoring and quantifying CO₂ emissions of isolated power plants from space. *Atmospheric Chemistry and Physics*, 23(11): 6599–6611
- Lindenmaier R, Dubey M K, Henderson B G, Butterfield Z T, Herman J R, Rahn T, Lee S H (2014). Multiscale observations of CO₂, ¹³CO₂, and pollutants at four corners for emission verification and attribution. *Proceedings of the National Academy of Sciences of the United States of America*, 111(23): 8386–8391
- Liu F, Beirle S, Zhang Q, D  rner S, He K, Wagner T (2016). NO_x lifetimes and emissions of cities and power plants in polluted background estimated by satellite observations. *Atmospheric Chemistry and Physics*, 16(8): 5283–5298
- Liu F, Duncan B N, Krotkov N A, Lamsal L N, Beirle S, Griffin D, McLinden C A, Goldberg D L, Lu Z (2020). A methodology to constrain carbon dioxide emissions from coal-fired power plants using satellite observations of co-emitted nitrogen dioxide. *Atmospheric Chemistry and Physics*, 20(1): 99–116
- Liu J, Bowman K W, Schimel D S, Parazoo N C, Jiang Z, Lee M, Bloom A A, Wunch D, Frankenberg C, Sun Y, et al. (2017). Contrasting carbon cycle responses of the tropical continents to the 2015–2016 El Ni  o. *Science*, 358(6360): eaam5690
- Liu S, Valks P, Curci G, Chen Y, Shu L, Jin J, Sun S, Pu D, Li X, Li J, et al. (2024). Satellite NO₂ retrieval complicated by aerosol composition over global urban agglomerations: seasonal variations and long-term trends (2001–2018). *Environmental Science & Technology*, 58(18): 7891–7903
- Liu Y, Wang J, Yao L, Chen X, Cai Z, Yang D, Yin Z, Gu S, Tian L, Lu N, et al. (2018). The TanSat mission: preliminary global observations. *Science Bulletin*, 63(18): 1200–1207
- Liu Z, Deng Z, Davis S, Ciais P (2023). Monitoring global carbon emissions in 2022. *Nature Reviews. Earth & Environment*, 4(4): 205–206
- Liu Z, Deng Z, Zhu B, Ciais P, Davis S J, Tan J, Andrew R M, Boucher O, Arous S B, Canadell J G, et al. (2022). Global patterns of daily CO₂ emissions reductions in the first year of COVID-19. *Nature Geoscience*, 15(8): 615–620
- Lu X, Ye X, Zhou M, Zhao Y, Weng H, Kong H, Li K, Gao M, Zheng B, Lin J, et al. (2021). The underappreciated role of agricultural soil nitrogen oxide emissions in ozone pollution regulation in North China. *Nature Communications*, 12(1): 5021
- Luderer G, Madeddu S, Merfort L, Ueckerdt F, Pehl M, Pietzcker R, Rottoli M, Schreyer F, Bauer N, Baumstark L, et al. (2022). Impact of declining renewable energy costs on electrification in low-emission scenarios. *Nature Energy*, 7(1): 32–42
- MacDonald C G, Mastrogiacomo J P, Laughner J L, Hedelius J K, Nassar R, Wunch D (2023). Estimating enhancement ratios of nitrogen dioxide, carbon monoxide and carbon dioxide using satellite observations. *Atmospheric Chemistry and Physics*, 23(6): 3493–3516
- Maral G, De Ridder J J, Evans B G, Richharia M (1991). Low earth orbit satellite systems for communications. *International Journal of Satellite Communications*, 9(4): 209–225
- Martin R V, Jacob D J, Chance K, Kurosu T P, Palmer P I, Evans M J (2003). Global inventory of nitrogen oxide emissions constrained by space-based observations of NO₂ columns. *Journal of Geophysical Research*, 108(D17): 2003JD003453
- Massman W J (1998). A review of the molecular diffusivities of H₂O, CO₂, CH₄, CO, O₃, SO₂, NH₃, N₂O, NO, and NO₂ in air, O₂ and N₂ near STP. *Atmospheric Environment*, 32(6): 1111–1127
- Meinshausen M, Lewis J, Mcglade C, Gutschow J, Nicholls Z, Burdon R, Cozzi L, Hackmann B (2022). Realization of Paris Agreement pledges may limit warming just below 2   C. *Nature*, 604(7905): 304–309
- Miyazaki K, Bowman K (2023). Predictability of fossil fuel CO₂ from air quality emissions. *Nature Communications*, 14(1): 1604
- Miyazaki K, Eskes H, Sudo K, Boersma K F, Bowman K, Kanaya Y (2017). Decadal changes in global surface NO_x emissions from multi-constituent satellite data assimilation. *Atmospheric Chemistry and Physics*, 17(2): 807–837
- Moon J, Choi Y, Jeon W, Kim H C, Pouyaei A, Jung J, Pan S, Kim S, Kim C H, Bak J, et al. (2024). Hybrid IFDMB/4D-Var inverse modeling to constrain the spatiotemporal distribution of CO and NO₂ emissions using the CMAQ adjoint model. *Atmospheric Environment*, 327: 120490
- Nassar R, Hill T G, McLinden C A, Wunch D, Jones D B A, Crisp D (2017). Quantifying CO₂ Emissions from Individual Power Plants From Space. *Geophysical Research Letters*, 44(19): 10045–10053
- Nassar R, Mastrogiacomo J P, Bateman-Hemphill W, Mccracken C, Macdonald C G, Hill T, O'Dell C W, Kiel M, Crisp D (2021). Advances in quantifying power plant CO₂ emissions with OCO-2. *Remote Sensing of Environment*, 264: 112579
- Nassar R, Moeini O, Mastrogiacomo J P, O'Dell C W, Nelson R R, Kiel M, Chatterjee A, Eldering A, Crisp D (2022). Tracking CO₂ emission reductions from space: a case study at Europe's largest fossil fuel power plant. *Frontiers in Remote Sensing*, 3
- Nassar R, Napier-Linton L, Gurney K R, Andres R J, Oda T, Vogel

- F R, Deng F (2013). Improving the temporal and spatial distribution of CO₂ emissions from global fossil fuel emission data sets. *Journal of Geophysical Research. Atmospheres*, 118(2): 917–933
- Nehrkorn T, Eluszkiewicz J, Wofsy S C, Lin J C, Gerbig C, Longo M, Freitas S (2010). Coupled weather research and forecasting-stochastic time-inverted lagrangian transport (WRF–STILT) model. *Meteorology and Atmospheric Physics*, 107(1): 51–64
- Newman R, Noy I (2023). The global costs of extreme weather that are attributable to climate change. *Nature Communications*, 14(1): 6103
- Olsen S C, Randerson J T (2004). Differences between surface and column atmospheric CO₂ and implications for carbon cycle research. *Journal of Geophysical Research*, 109(D2): 2003JD003968
- Ombadi M, Risser M D, Rhoades A M, Varadharajan C (2023). A warming-induced reduction in snow fraction amplifies rainfall extremes. *Nature*, 619(7969): 305–310
- Palmer P I, Jacob D J, Fiore A M, Martin R V, Chance K, Kurosu T P (2003). Mapping isoprene emissions over North America using formaldehyde column observations from space. *Journal of Geophysical Research*, 108(D6): 2002JD002153
- Park H, Jeong S, Park H, Labzovskii L D, Bowman K W (2021). An assessment of emission characteristics of Northern Hemisphere cities using spaceborne observations of CO₂, CO, and NO₂. *Remote Sensing of Environment*, 254: 112246
- Park S S, Kozawa K, Fruin S, Mara S, Hsu Y K, Jakober C, Winer A, Herner J (2011). Emission Factors for high-emitting vehicles based on on-road measurements of individual vehicle exhaust with a mobile measurement platform. *Journal of the Air & Waste Management Association*, 61(10): 1046–1056
- Penn E, Holloway T (2020). Evaluating current satellite capability to observe diurnal change in nitrogen oxides in preparation for geostationary satellite missions. *Environmental Research Letters*, 15(3): 034038
- Pillai D, Buchwitz M, Gerbig C, Koch T, Reuter M, Bovensmann H, Marshall J, Burrows J P (2016). Tracking city CO₂ emissions from space using a high-resolution inverse modelling approach: a case study for Berlin, Germany. *Atmospheric Chemistry and Physics*, 16(15): 9591–9610
- Qu Z, Henze D K, Worden H M, Jiang Z, Gaubert B, Theys N, Wang W (2022). Sector-based top-down estimates of NO_x, SO₂, and CO emissions in East Asia. *Geophysical Research Letters*, 49(2): e2021GL096009
- Reuter M, Buchwitz M, Hilboll A, Richter A, Schneising O, Hilker M, Heymann J, Bovensmann H, Burrows J P (2014). Decreasing emissions of NO_x relative to CO₂ in East Asia inferred from satellite observations. *Nature Geoscience*, 7(11): 792–795
- Reuter M, Buchwitz M, Schneising O, Krautwurst S, O'Dell C W, Richter A, Bovensmann H, Burrows J P (2019). Towards monitoring localized CO₂ emissions from space: co-located regional CO₂ and NO₂ enhancements observed by the OCO-2 and S5P satellites. *Atmospheric Chemistry and Physics*, 19(14): 9371–9383
- Röser F, Widerberg O, Höhne N, Day T (2020). Ambition in the making: analysing the preparation and implementation process of the Nationally Determined Contributions under the Paris Agreement. *Climate Policy*, 20(4): 415–429
- Santaren D, Broquet G, Bréon F M, Chevallier F, Siméoni D, Zheng B, Ciais P (2021). A local- to national-scale inverse modeling system to assess the potential of spaceborne CO₂ measurements for the monitoring of anthropogenic emissions. *Atmospheric Measurement Techniques*, 14(1): 403–433
- Schneising O, Buchwitz M, Reuter M, Heymann J, Bovensmann H, Burrows J P (2011). Long-term analysis of carbon dioxide and methane column-averaged mole fractions retrieved from SCIAMACHY. *Atmospheric Chemistry and Physics*, 11(6): 2863–2880
- Schuit B J, Maasakkers J D, Bijl P, Mahapatra G, Van Den Berg A W, Pandey S, Lorente A, Borsdorff T, Houweling S, Varon D J, et al. (2023). Automated detection and monitoring of methane super-emitters using satellite data. *Atmospheric Chemistry and Physics*, 23(16): 9071–9098
- Schwandner F M, Gunson M R, Miller C E, Carn S A, Eldering A, Krings T, Verhulst K R, Schimel D S, Nguyen H M, Crisp D, et al. (2017). Spaceborne detection of localized carbon dioxide sources. *Science*, 358(6360): eaam5782
- Shah V, Jacob D J, Dang R, Lamsal L N, Strode S A, Steenrod S D, Boersma K F, Eastham S D, Fritz T M, Thompson C, et al. (2023). Nitrogen oxides in the free troposphere: implications for tropospheric oxidants and the interpretation of satellite NO₂ measurements. *Atmospheric Chemistry and Physics*, 23(2): 1227–1257
- Shen L, Gao T, Zhao J, Wang L, Wang L, Liu L, Chen F, Xue J (2014). Factory-level measurements on CO₂ emission factors of cement production in China. *Renewable & Sustainable Energy Reviews*, 34: 337–349
- Shi Q, Zheng B, Zheng Y, Tong D, Liu Y, Ma H, Hong C, Geng G, Guan D, He K, et al. (2022). Co-benefits of CO₂ emission reduction from China's clean air actions between 2013–2020. *Nature Communications*, 13(1): 5061
- Silva S J, Arellano A F (2017). Characterizing regional-scale combustion using satellite retrievals of CO, NO₂ and CO₂. *Remote Sensing*, 9(7): 744
- Singh L A, Whittecar W R, Diprinzio M D, Herman J D, Furrer M P, Reed P M (2020). Low cost satellite constellations for nearly continuous global coverage. *Nature Communications*, 11(1): 200
- Solazzo E, Crippa M, Guizzardi D, Muntean M, Choulga M, Janssens-Maenhout G (2021). Uncertainties in the emissions database for global atmospheric research (EDGAR) emission inventory of greenhouse gases. *Atmospheric Chemistry and Physics*, 21(7): 5655–5683
- Squadrato G L, Pryor W A (1998). Oxidative chemistry of nitric oxide: the roles of superoxide, peroxyxynitrite, and carbon dioxide. *Free Radical Biology & Medicine*, 25(4–5): 392–403

- Stavrakou T, Müller J F, Boersma K F, de Smedt I, van der A R J (2008). Assessing the distribution and growth rates of NO_x emission sources by inverting a 10-year record of NO_2 satellite columns. *Geophysical Research Letters*, 35(10): 2008GL033521
- Sun Y, Frankenberg C, Wood J D, Schimel D S, Jung M, Guanter L, Drewry D T, Verma M, Porcar-Castell A, Griffiths T J, et al. (2017). OCO-2 advances photosynthesis observation from space via solar-induced chlorophyll fluorescence. *Science*, 358(6360): eaam5747
- Suto H, Kataoka F, Kikuchi N, Knuteson R O, Butz A, Haun M, Buijs H, Shiomi K, Imai H, Kuze A (2021). Thermal and near-infrared sensor for carbon observation Fourier transform spectrometer-2 (TANSO-FTS-2) on the Greenhouse gases Observing SATellite-2 (GOSAT-2) during its first year in orbit. *Atmospheric Measurement Techniques*, 14(3): 2013–2039
- Swain D L, Singh D, Touma D, Diffenbaugh N S (2020). Attributing Extreme events to climate change: a new frontier in a warming world. *One Earth*, 2(6): 522–527
- Tang L, Jia M, Yang J, Li L, Bo X, Mi Z (2023). Chinese industrial air pollution emissions based on the continuous emission monitoring systems network. *Scientific Data*, 10(1): 153
- Taylor T E, O'Dell C W, Baker D, Bruegge C, Chang A, Chapsky L, Chatterjee A, Cheng C, Chevallier F, Crisp D, et al. (2023). Evaluating the consistency between OCO-2 and OCO-3 XCO_2 estimates derived from the NASA ACOS version 10 retrieval algorithm. *Atmospheric Measurement Techniques*, 16(12): 3173–3209
- Thompson D, Brown T D, Beér J M (1972). NO_x formation in combustion. *Combustion and Flame*, 19(1): 69–79
- Thoning K W, Tans P P, Komhyr W D (1989). Atmospheric carbon dioxide at Mauna Loa Observatory: 2. Analysis of the NOAA GMCC data, 1974–1985. *Journal of Geophysical Research*, 94(D6): 8549–8565
- Tibrewal K, Ciais P, Saunio M, Martinez A, Lin X, Thanwerdas J, Deng Z, Chevallier F, Giron C, Albergel C, et al. (2024). Assessment of methane emissions from oil, gas and coal sectors across inventories and atmospheric inversions. *Communications Earth & Environment*, 5(1): 26
- Turner A J, Henze D K, Martin R V, Hakami A (2012). The spatial extent of source influences on modeled column concentrations of short-lived species. *Geophysical Research Letters*, 39(12): 2012GL051832
- Ulybyshev Y (2008). Satellite constellation design for complex coverage. *Journal of Spacecraft and Rockets*, 45(4): 843–849
- van Geffen J, Boersma K F, Eskes H, Sneep M, Ter Linden M, Zara M, Veefkind J P (2020). S5P TROPOMI NO_2 slant column retrieval: method, stability, uncertainties and comparisons with OMI. *Atmospheric Measurement Techniques*, 13(3): 1315–1335
- van Geffen J, Eskes H, Compernelle S, Pinardi G, Verhoelst T, Lambert J C, Sneep M, Ter Linden M, Ludewig A, Boersma K F, et al. (2022). Sentinel-5P TROPOMI NO_2 retrieval: impact of version v2.2 improvements and comparisons with OMI and ground-based data. *Atmospheric Measurement Techniques*, 15(7): 2037–2060
- Vance T C, Huang T, Butler K A (2024). Big data in Earth science: emerging practice and promise. *Science*, 383(6688): eadh9607
- Veefkind J P, Aben I, McMullan K, Förster H, de Vries J, Otter G, Claas J, Eskes H J, de Haan J F, Kleipool Q, et al. (2012). TROPOMI on the ESA Sentinel-5 Precursor: a GMES mission for global observations of the atmospheric composition for climate, air quality and ozone layer applications. *Remote Sensing of Environment*, 120: 70–83
- Velasco V A, Buchwitz M, Bovensmann H, Reuter M, Schneising O, Heymann J, Krings T, Gerilowski K, Burrows J P (2011). Towards space based verification of CO_2 emissions from strong localized sources: fossil fuel power plant emissions as seen by a CarbonSat constellation. *Atmospheric Measurement Techniques*, 4(12): 2809–2822
- Wang H, Jiang F, Wang J, Ju W, Chen J M (2019). Terrestrial ecosystem carbon flux estimated using GOSAT and OCO-2 XCO_2 retrievals. *Atmospheric Chemistry and Physics*, 19(18): 12067–12082
- Wei J, Liu S, Li Z, Liu C, Qin K, Liu X, Pinker R T, Dickerson R R, Lin J, Boersma K F, et al. (2022). Ground-Level NO_2 Surveillance from space across China for high resolution using interpretable spatiotemporally weighted artificial intelligence. *Environmental Science & Technology*, 56(14): 9988–9998
- Weir B, Crisp D, O'Dell C W, Basu S, Chatterjee A, Kolassa J, Oda T, Pawson S, Poulter B, Zhang Z, et al. (2021). Regional impacts of COVID-19 on carbon dioxide detected worldwide from space. *Science Advances*, 7(45): eabf9415
- Winker D M, Vaughan M A, Omar A, Hu Y, Powell K A, Liu Z, Hunt W H, Young S A (2009). Overview of the CALIPSO mission and CALIOP data processing algorithms. *Journal of Atmospheric and Oceanic Technology*, 26(11): 2310–2323
- Wren S N, McLinden C A, Griffin D, Li S M, Cober S G, Darlington A, Hayden K, Mihele C, Mittermeier R L, Wheeler M J, et al. (2023). Aircraft and satellite observations reveal historical gap between top-down and bottom-up CO_2 emissions from Canadian oil sands. *PNAS Nexus*, 2(5): pgad140
- Wu D, Lin J C, Fasoli B, Oda T, Ye X, Lauvaux T, Yang E G, Kort E A (2018). A Lagrangian approach towards extracting signals of urban CO_2 emissions from satellite observations of atmospheric column CO_2 (XCO_2): X-Stochastic Time-Inverted Lagrangian Transport model ("X-STILT v1"). *Geoscientific Model Development*, 11(12): 4843–4871
- Wu D, Lin J C, Oda T, Kort E A (2020). Space-based quantification of per capita CO_2 emissions from cities. *Environmental Research Letters*, 15(3): 035004
- Xu R, Tong D, Davis S J, Qin X, Cheng J, Shi Q, Liu Y, Chen C, Yan L, Yan X, et al. (2023). Plant-by-plant decarbonization strategies for the global steel industry. *Nature Climate Change*, 13(10): 1067–1074
- Xu T, Zhang C, Xue J, Hu Q, Xing C, Liu C (2024). Estimating hourly nitrogen oxide emissions over East Asia from geostationary satellite measurements. *Environmental Science &*

- Technology Letters, 11(2): 122–129
- Yang D, Boesch H, Liu Y, Somkuti P, Cai Z, Chen X, Di Noia A, Lin C, Lu N, Lyu D, et al. (2020). Toward high precision XCO₂ retrievals from tansat observations: retrieval improvement and validation against TCCON measurements. *Journal of Geophysical Research: Atmospheres*, 125(22): e2020JD032794
- Yang D, Liu Y, Cai Z, Chen X, Yao L, Lu D (2018). First global carbon dioxide maps produced from TanSat measurements. *Advances in Atmospheric Sciences*, 35(6): 621–623
- Yang E G, Kort E A, Ott L E, Oda T, Lin J C (2023). Using space-based CO₂ and NO₂ observations to estimate urban CO₂ emissions. *Journal of Geophysical Research: Atmospheres*, 128(6): e2022JD037736
- Yang J, Gong P, Fu R, Zhang M, Chen J, Liang S, Xu B, Shi J, Dickinson R (2013). The role of satellite remote sensing in climate change studies. *Nature Climate Change*, 3(10): 875–883
- Ye X, Lauvaux T, Kort E A, Oda T, Feng S, Lin J C, Yang E G, Wu D (2020). Constraining fossil fuel CO₂ emissions from urban area using OCO-2 observations of total column CO₂. *Journal of Geophysical Research: Atmospheres*, 125(8): e2019JD030528
- Yuan X, Wang Y, Ji P, Wu P, Sheffield J, Otkin J A (2023). A global transition to flash droughts under climate change. *Science*, 380(6641): 187–191
- Zhang C, Liu C, Chan K L, Hu Q, Liu H, Li B, Xing C, Tan W, Zhou H, Si F, et al. (2020). First observation of tropospheric nitrogen dioxide from the environmental trace gases monitoring instrument onboard the GaoFen-5 satellite. *Light, Science & Applications*, 9(1): 66
- Zhang Q, Boersma K F, Zhao B, Eskes H, Chen C, Zheng H, Zhang X (2023). Quantifying daily NO_x and CO₂ emissions from Wuhan using satellite observations from TROPOMI and OCO-2. *Atmospheric Chemistry and Physics*, 23(1): 551–563
- Zhao C, Wang Y (2009). Assimilated inversion of NO_x emissions over east Asia using OMI NO₂ column measurements. *Geophysical Research Letters*, 36(6): 2008GL037123
- Zhao H, He W, Cheng J, Liu Y, Zheng Y, Tian H, He K, Lei Y, Zhang Q (2024). Heterogeneities in regional air pollutant emission mitigation across China during 2012–2020. *Earth's Future*, 12(3): e2023EF004139
- Zheng B, Chevallier F, Ciais P, Broquet G, Wang Y, Lian J, Zhao Y (2020a). Observing carbon dioxide emissions over China's cities and industrial areas with the Orbiting Carbon Observatory-2. *Atmospheric Chemistry and Physics*, 20(14): 8501–8510
- Zheng B, Ciais P, Chevallier F, Yang H, Canadell J G, Chen Y, van der Velde I R, Aben I, Chuvieco E, Davis S J, et al. (2023). Record-high CO₂ emissions from boreal fires in 2021. *Science*, 379(6635): 912–917
- Zheng B, Geng G, Ciais P, Davis S J, Martin R V, Meng J, Wu N, Chevallier F, Broquet G, Boersma F, et al. (2020b). Satellite-based estimates of decline and rebound in China's CO₂ emissions during COVID-19 pandemic. *Science Advances*, 6(49): eabd4998
- Zheng B, Tong D, Li M, Liu F, Hong C, Geng G, Li H, Li X, Peng L, Qi J, et al. (2018). Trends in China's anthropogenic emissions since 2010 as the consequence of clean air actions. *Atmospheric Chemistry and Physics*, 18(19): 14095–14111
- Zheng B, Zhang Q, Tong D, Chen C, Hong C, Li M, Geng G, Lei Y, Huo H, He K (2017). Resolution dependence of uncertainties in gridded emission inventories: a case study in Hebei, China. *Atmospheric Chemistry and Physics*, 17(2): 921–933
- Zheng T, Nassar R, Baxter M (2019). Estimating power plant CO₂ emission using OCO-2 XCO₂ and high resolution WRF-Chem simulations. *Environmental Research Letters*, 14(8): 085001
- Zhu X, Gao Y (2017). Comparison of intelligent algorithms to design satellite constellations for enhanced coverage capability. In: *Proceedings of the 10th International Symposium on Computational Intelligence and Design (ISCID)*, Hangzhou, China
- Zoogman P, Liu X, Suleiman R M, Pennington W F, Flittner D E, Al-Saadi J A, Hilton B B, Nicks D K, Newchurch M J, Carr J L, et al. (2017). Tropospheric emissions: monitoring of pollution (TEMPO). *Journal of Quantitative Spectroscopy & Radiative Transfer*, 186: 17–39
- zu Castell W, Ruhnke R, Bouwer L M, Brix H, Dietrich P, Dransch D, Frickenhaus S, Greinert J, Petzold A (2022). *Integrating Data Science and Earth Science: Challenges and Solutions*. Berlin: Springer International Publishing

Author Biography



Bo Zheng is an associate professor at Tsinghua Shenzhen International Graduate School. He received B.S. and Ph.D. degrees from Tsinghua University in Environmental Engineering. Then he completed a four-year post-doctoral training at the Laboratory for Sciences of Climate and Environment in France before joining Tsinghua Shenzhen International Graduate School as an Assistant Professor in 2021. He focuses on the atmospheric carbon cycle and has developed a variety of techniques to analyze the sources and sinks of atmospheric constituents (e.g., greenhouse gases and air pollutants) based on satellite remote sensing. He has published over 150 peer-reviewed articles, which have received over 27000 times citations with an H-index of 66 (Google scholar).